Two-pore domain K^+ channel TASK-1 in human pulmonary artery smooth muscle cells and its regulation by the vasoconstrictor endothelin-1

Inauguraldissertation

Zur Erlangung des Grades eines Doktors der Medizin

des Fachbereichs Medizin

der Justus-Liebig Universität Giessen

vorgelegt von Tang, Bi MD

aus Ling Bi, Anhui province, China

Gießen, 2010

Aus dem Zentrum für Innere Medizin, Medizinische Klinik und Poliklinik II,
Pneumologie und Intensivmedizin
Direktor: Prof. Dr. Werner Seeger

Gutachter: Prof. DDr. T. Braun
Gutachter: Prof. Dr. A. Olschewski

Tag der Disputation: 06. 07. 2010

My wife, Pingping Sun,

for her constant interest and her continuous helpfulness

My family for the continuous support and

encouragement during my doctoral dissertation

Table of contents

Abbreviation:

DAG: diacylglycerol

EGTA: ethyleneglycol bis(ß-aminoethyl ether)-*N*,*N*,*N*',*N*'-tetraacetic acid

$\mathbf{E_m}$: resting membrane potential

ET-1: endothelin-1

FITC: fluorescein isothiocyanate-conjugated

HEPES: 4-(2-Hydroxyethyl) piperazine-1-ethanesulfonic acid

HPV: hypoxic pulmonary vasoconstriction

$\boldsymbol{I_{KN}}$: noninactivating K^+ current

$\mathbf{K_{ATP}}$: ATP-sensitive potassium channels

$\mathbf{K_{2P}}$: two-pore domain potassium (K^+) channels

KCa: calcium-activated potassium channels

$\mathbf{K_V}$: voltage-dependent potassium channels

PH: pulmonary hypertension

PAH: pulmonary arterial hypertension

PAP: pulmonary arterial pressure

PASMC: pulmonary arterial smooth muscle cell

PCR: polymerase chain reaction

pHo: extracellular pH

$\mathbf{PIP_2}$: phosphatidylinositol 4,5-biphosphate

PKA: protein kinase A

PKC: protein kinase C

PLC: phospholipase C

siRNA: small interfering RNA

TASK-1: TWIK-related acid-sensitive K^+; TWIK, for tandem P domains in a weak inwardly rectifying K^+

TEA: tetraethylammonium

1. Introduction and question

The membrane potential of pulmonary vascular smooth muscle cells is a key regulator of the arterial tone. These cells have a resting membrane potential of approximately -65 to -50 mV in vitro, close to the predicted equilibrium potential for potassium (K^+) ions. Thereby, the vasodilator effect of agents that induces the K^+ channels opening in the pulmonary arterial smooth muscle cell (PASMC) membrane increases the K^+ efflux, which in turn results in membrane hyperpolarization. Due to this hyperpolarization, the voltage-dependent Ca^{2+} channels are closed, which decreases the Ca^{2+} entry and leads to vasodilatation (Clapp *et al.*, 1993), (Wanstall, 1996). Conversely, the vasoconstrictor action of drugs inhibits K^+ channels causing membrane depolarization, Ca^{2+} entry, cell contraction, and finally vasoconstriction (Hara *et al.*, 1980),(Hasunuma *et al.*, 1991),(Post *et al.*, 1992).

Background or leak K^+-selective channels, as defined by a lack of time and voltage dependency, play an essential role in setting the resting membrane potential and input resistance in excitable cells. These channels are structurally unique in that each subunit possesses four transmembrane segments and two pore-forming domains and hence are often referred to as two-pore domain K^+ channels. Two-pore domain K^+ (2-PK) channels have been shown to conduct several leak K^+ currents. The activity of 2-PK channels is strongly regulated by numerous chemical and physical physiological stimuli, such as extracelluar pH, protons, protein kinases, phospholipids, neurotransmitters, volatile anesthetics and hypoxia (Gurney *et al.*, 2009). An alteration of the K^+ conductance can influence the cellular activity via membrane potential changes.

Both, RT-PCR and Northern blot analyses using mammalian lung tissue have identified mRNA transcripts for several 2-PK channels (Medhurst *et al.*, 2001),(Duprat *et al.*, 1997),(Lesage *et al.*, 2000). Recently, TASK-1 (TWIK-related acid-sensitive K^+ ;TWIK, for tandem P domains in a weak inwardly rectifying K^+), a member of the 2-PK channel family has been described in rabbit PASMC (Gurney *et al.*, 2003) as well as in rat pulmonary arteries (Gardener *et al.*, 2004). This channel produces K^+ currents that

possess all of the characteristics of background conductances. The activity of TASK-1 is strongly dependent on the external pH and oxygen tension, suggesting that this particular channel might be a sensor of external pH variations and of hypoxia in pulmonary arteries.

The present report demonstrates the expression of TASK-1 in human PASMC. Our study has tested the hypothesis that TASK-1 contributes to the K^+ current and resting membrane potential by using TASK-1 small interfering RNA (siRNA). Moreover, we show that TASK-1 is reversibly inhibited by acute hypoxia, which is compatible with it being responsible for the oxygen sensitivity of the membrane potential.

Endothelin-1 (ET-1), a 21-amino-acid peptide secreted by vascular endothelial cells, is the most potent vasoconstrictor described to date (Yanagisawa *et al.*, 1988) and is considered to be a major player within the pathological mechanisms involved in pulmonary arterial hypertension (PAH) (Stewart *et al.*, 1991),(Giaid *et al.*, 1993). ET-1 causes long-lasting vasoconstriction(Yanagisawa *et al.*, 1988) and excessive proliferation in pulmonary artery smooth muscle cells (Hirata *et al.*, 1989),(Wort *et al.*, 2001),(Davie *et al.*, 2002), contributing to vascular remodeling. Multiple lines of evidences show that ET-1 plays a central role in the pathogenesis of pulmonary arterial hypertension (PAH) (Hynynen *et al.*, 2006),(Galie *et al.*, 2004),(Galie *et al.*, 2004),(Giaid *et al.*, 1993),(Rubin *et al.*, 2002),(Chen *et al.*, 1995). K^+ channels determine the membrane potential of PASMCs and represent an important controller of their calcium homeostasis (Yuan, 1995),(Olschewski *et al.*, 2002). Furthermore, it is now well established that an inhibition of K^+ channels e.g. by serotonin or hypoxia causes membrane depolarization and stimulates PASMC proliferation (Weir *et al.*, 2006),(Yu *et al.*, 2001),(Eddahibi *et al.*, 2006). Several reports indicate that TASK-1 plays an important role in human pulmonary circulation. The TASK-1 channel contributes substantially to the K^+ conductance and sets resting membrane potential in PASMCs (Gurney *et al.*, 2003),(Gardener *et al.*, 2004), where other K^+ channels like voltage-gated (K_V) or calcium-dependent K^+ channels are not activated. Moreover, TASK-1 is modulated by extracelluar pH, protein kinases, hypoxia or vasoactive factors such as prostacyclin (Duprat *et al.*, 1997),(Buckler *et al.*, 2000). Furthermore, the

two-pore K^+ domain channels are supposed to be involved in hypoxic pulmonary vasoconstriction (Gurney *et al.*, 2006).

Based on their properties, both TASK-1 channels and ET-1 might interact in the pathogenesis of PAH. Although numerous studies have investigated ion channels in PAH, the TASK-1 in human PASMC has not been taken into account until now. Considering the features of TASK-1, we have hypothesized that ET-1 might inhibit TASK-1 channels. In particular, to date, the molecular signaling mechanism for inhibition of TASK-1 in native human cells is poorly understood. Therefore, in the present study, we have investigated the signaling pathway and the effects of ET-1 on TASK-1 in primary human PASMCs and found the pathway from ET_A receptors, through phospholipase C (PLC), phosphatidylinositol 4,5-biphosphate (PIP_2), diacylglycerol (DAG) and protein kinase C (PKC) to TASK-1.

Papers publishing the results of this work

Olschewski, A; Li, Y; **Tang, B**; Hanze, J; Eul, B; Bohle, RM; Wilhelm, J; Morty, RE; Brau, ME; Weir, EK; Kwapiszewska, G; Klepetko, W; Seeger, W; Olschewski, H: Impact of TASK-1 in human pulmonary artery smooth muscle cells. *Circ Res*. 2006; 98(8): 1072-1080.

Tang, B; Li, Y; Nagaraj, C; Morty, RE; Gabor, S; Stacher, E; Voswinckel, R; Weissmann, N; Leithner, K; Olschewski, H; Olschewski, A: Endothelin-1 inhibits background two-pore domain channel TASK-1 in primary human pulmonary artery smooth muscle cells. *Am J Respir Cell Mol Biol*. 2009; 41(4):476-483.

Abstracts publishing the results of this work

Tang, B; Li, Y; Haenze, J; Eul, B; Morty, RE; Olschewski, A; Olschewski, H The two-pore domain K^+ channel TASK-1 is blocked by endothelin-1 in human pulmonary artery smooth muscle cells. *Med Klin*.; 101: A83-A83.-DGIM; APR 22-26, 2006; Wiesbaden, Germany.

Li, Y; **Tang, B**; Hanze, J; Eul, B; Bohle, RM; Wilhelm, J; Morty, RE; Weir, EK; Klepetko, W; Olschewski, A; Olschewski, H: The two-pore domain K^+ channel TASK-1 largely contributes to resting membrane potential in human pulmonary artery smooth muscle cells *Med Klin*.; 101: A83-A83.-DGIM; APR 22-26, 2006; Wiesbaden, Germany.

Tang, B; Li, Y; Morty, RE; Hanze, J; Eul, B; Olschewski, H; Olschewski, A: The two-pore domain K^+ channel TASK-1 is blocked by endothelin-1 in human pulmonary artery smooth muscle cells. *Proceedings of the American Thoracic Society (PATS)*.

3(4):A691--International Conference of the American Thoracic Society 2006; 19-24. 05. 2006; San Diego, USA.

Li, Y; Hanze, J; **Tang, B**; Eul, B; Bohle, RM; Wilhelm, J; Morty, RE; Weir, EK; Olschewski, H; Olschewski, A: The Two-Pore Domain K^+ Channel TASK-1 Largerly Contributes to Resting Membrane Potential in Human Pulmonary Artery Smooth Muscle Cells. *Proceedings of the American Thoracic Society (PATS).* 3(4):A855--International Conference of American Thoracic Society 2006; 19-24, 05, 2006; San Diego, USA.

Tang, B; Li, Y; Leithner, K ; Morty, RE; Hanze, J; Eul, B; Olschewski, H; Olschewski, A: The two-pore domain K^+ channel TASK-1 is modulated by endothelin-1 in human pulmonary artery smooth muscle cells. *ÖGP Jahrestagung*; NOV 6-9, 2006; Graz, Austria.

Tang, B; L i, Y; Nagaraj, C; Leithner, K; Gabor, S; Popper, H; Olschewski, H; Olschewski, A: TASK-1 Inhibition in Human Pulmonary Artery Smooth Muscle Cells by Endothelin-1 Is Mediated by a Phospholipase C-Diacylglycerol-Protein Kinase C-Pathway. *American Journal of Respiratory and Critical Care Medicine*_2008; 177: A926--International Conference of the American Thoracic Society; MAY 16-21, 2008; Toronto, Canada.

Tang, B; Li, Y; Nagaraj, C; Leithner, K; Gabor, S; Popper, H; Olschewski, H; Olschewski, A: Endothelin-1 inhibits TASK-1 in Human Pulmonary Artery Smooth Muscle Cells via a Phospholipase C-Diacylglycerol-Protein Kinase C-Pathway. *European Respiratory Journal*_2008; 32(S52):27s--Annual Congress of the European Respiratory Society; OCT 4-8, 2008; Berlin, Germany.

Nagaraj, C; **Tang, B**; Bálint, Z; Lindenmann, J; Stacher, E; Olschewski, A Molecular mechanisms behind the acute oxygen sensing of potassium channels in primary human pulmonary artery smooth muscle cells. *Physiology*_2009; JUL 7-11, 2009; Dublin, Ireland. 2009.

2. Potassium channels in human PASMCs

The potassium current in PASMCs is an ensemble, reflecting activity of many different channels. At least three classes of potassium channels have been identified in PASMCs: voltage-dependent potassium channels (Kv) (Yuan, 1995),(Post *et al.*, 1995),(Evans *et al.*, 1996), calcium-activated potassium channels (K_{Ca}) (Albarwani *et al.*, 1994),(Peng *et al.*, 1999) and ATP-sensitive potassium channels (K_{ATP}) (Nelson *et al.*, 1995). The potassium channels which control the resting membrane potential (E_m) in PASMCs, and inhibition of which initiates hypoxic pulmonary vasoconstriction (HPV), conduct an outward current which is slowly inactivated and blocked by the Kv channel blocker 4-aminopyridine (4-AP) but not by inhibitors of K_{Ca} or K_{ATP}, at least in the rat (Yuan, 1995),(Archer *et al.*, 1996),(Archer *et al.*, 1998). At the molecular level, Kv channels are homo- or heteromultimeric tetramers composed of two structural distinct subunits: the pore forming α-subunits and the regulatory β-subunits (Hille, 1986). Nine families of Kv channel α-subunits are recognized from cloning studies (Kv1-9) (Hille, 1986),(Pongs, 1992), each with subtypes (e.g. Kv1.1-1.6). The molecular identification of the specific Kv channels that control E_m is difficult, even with advanced electrophysiological techniques, mainly due to lack of specific blockers. However, the intracellular dialysis of specific Kv antibodies combined with patch-clamp recordings, studies in expression systems, or the use of reverse transcription polymerase chain reaction (PCR) may throw light on the involvement of K^+ channels in the mechanism of HPV. The potential candidate Kv channel α-subunits that could form O_2-sensitive channels in PA SMCs are Kv1.2 (Wang *et al.*, 1997),(Hulme *et al.*, 1999) , Kv1.5 (Archer *et al.*, 1998),(Wang *et al.*, 1997), Kv2.1 (Archer *et al.*, 1998),(Hulme *et al.*, 1999),(Patel *et al.*, 1997), Kv3.1 (Osipenko *et al.*, 1997) and Kv9.3 (Hulme *et al.*, 1999),(Patel *et al.*, 1997).

3. Background two-pore domain potassium channels (K_{2P})

Background or leak K^+-selective channels, as defined by a lack of time and voltage dependency, play an essential role in setting the resting membrane potential and input resistance in excitable cells. Alteration of the K^+ conductance in these cells influences the cellular activity via membrane potential changes. Two-pore domain K^+ (K_{2P}) channels have been shown to conduct several leak K^+ currents. This new gene family of K^+ channels has been progressively identified over the last few years (Bayliss *et al.*, 2001). Members of the KCNK family present structural features that suggest a dimeric arrangement, with each subunit comprising four transmembrane segments and two pore-forming regions (Fig. 1A). The channels formed by members of this family are distinct from voltage-dependent or inwardly rectifying K^+ channels in so far as most are constitutively active at resting membrane potentials and generate currents that rectify only very weakly. They can be grouped into six subfamilies based on their structural and functional properties in mammals: the TWIK (TWIK1, TWIK2, KCNK7), TASK (TASK1, TASK3, TASK5), TREK (TREK1, TREK2, TRAAK), TALK (TALK1, TALK2, TASK2), THIK (THIK1, THIK2) and TRESK subfamilies (Goldstein *et al.*, 1998),(O'Connell *et al.*, 2002).

K_{2P} channels are found in neuronal and non-neuronal tissues providing a wide variety of important functions, including the sensing of oxygen and pH (Patel *et al.*, 2001), the setting of resting membrane potentials (Kim *et al.*, 1998),(Millar *et al.*, 2000), the sensing of changes in $[K^+]$, the responses to agonists (Kim, 2003), neuroprotection (Buckler *et al.*, 2005) and mechanosensitivity (Kim, 2003),(Chemin *et al.*, 2005). K_{2P} channels are also candidates for the action of volatile anesthetics on neural excitability (Buckingham *et al.*, 2005). Most detailed information about the function of these channels comes from studies on cloned channels heterologously expressed in model cells.

TASK-1 and TASK-3, along with the silent subunit TASK-5, form a distinct structural and functional subgroup. The TASK-1 amino acid sequence shares 54% identity with TASK-3. The heteromultimerization between both subunits has been demonstrated

(Kang *et al.*, 2004),(Czirjak *et al.*, 2002). TASK-1 is a two-pore domain K^+ channel that generates a pH-sensitive, weakly-rectifying K^+ current (Duprat *et al.*, 1997),(Leonoudakis *et al.*, 1998),(Kim *et al.*, 1998). TASK-1 is called an 'open rectifier' because it exhibits no time-dependence and/or extremely fast kinetics (Lopes *et al.*, 2000). The current-to-voltage relationship of TASK channels becomes linear in a symmetrical K^+ gradient (reversing at 0 mV). This typical channel behavior is expected of a K^+-selective leak channel, as predicted by the Goldman-Hodgkin-Katz formulation (open rectifier). The homomultimers TASK-1, TASK-3 and the heteromultimer TASK-1–TASK-3 have single-channel conductances (determined in a symmetrical K^+ gradient) of 14 pS, 37 pS and 38 pS, respectively and are characterized by a typical flickery gating (Czirjak *et al.*, 2002),(Han *et al.*, 2002).

Several studies have inferred that K_{2P} channels may be involved in important cerebellar functions, such as spatial determination and accuracy, motor coordination, balance, muscle tone, and learning of motor skills. In other regions of the brain, K_{2P} channels, such as TASK-1 and TASK-3, are expressed and may function in behavior such as sleep and wakefulness, contribute to background conductance, and provide acid and volatile anesthetics sensitivity (Meuth *et al.*, 2003). In contrast, there have been limited reports of K_{2P} channels in cardiac or smooth muscle tissues. Due to TASK-1 cardiac myocytes display a background K^+ current, (Kim *et al.*, 1998), influencing the amplitude and duration of action potentials (Backx *et al.*, 1993). Smooth muscle cells in the carotid body express TASK-3. Another group has reported expression of TASK and TREK isoforms in human myometrium using RT-PCR. Western analyses have showed the expression of TASK-1 and TREK-1 in this tissue (Bai *et al.*, 2005). Subsequently, Sanders & Koh have found expression and function of TASK and TREK channels in gastrointestinal smooth muscle cells (Sanders *et al.*, 2006). Their findings support the role of TASK-1 in the regulation of gastrointestinal smooth muscles. In addition, TASK-1 channels appear to participate in establishing the moment-to-moment state of excitability in gastrointestinal muscles. Finally, there exist an evidence that TASK-1 maintains the resting potential in bladder smooth muscles (Beckett *et al.*, 2008). The relevance of TASK-1 in vascular smooth muscle cells with special focus on the

pulmonary arteries is described in the next section.

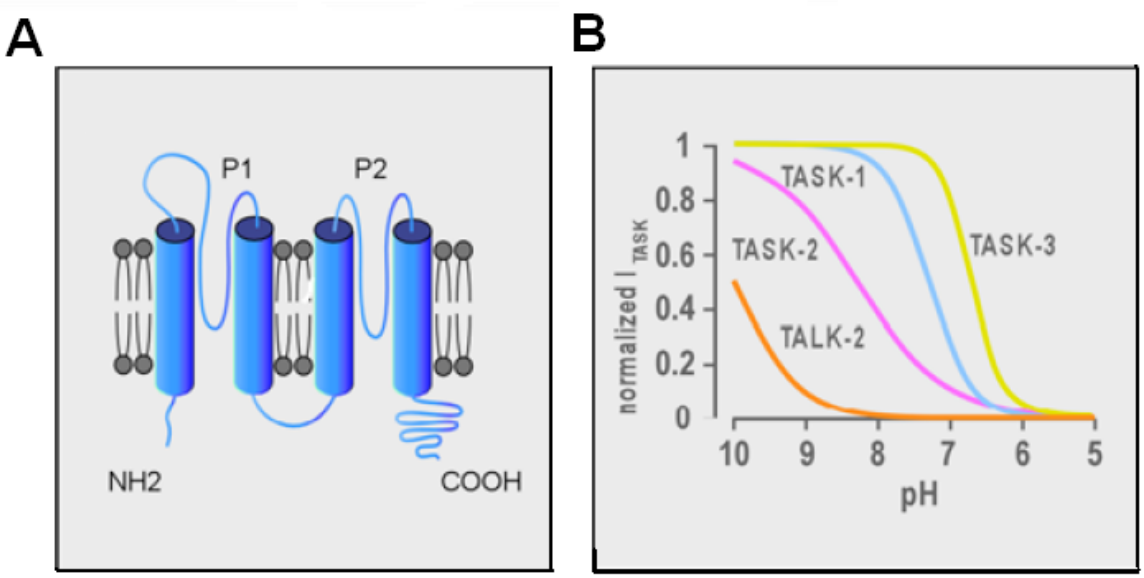

Fig. 1: Topology and pharmacology of K_{2P} channels. (from Patel *et al.*, 2004)

A: 2P-domain K^+ channels consist of four transmembrane segments and two pores in tandem, P1 and P2. A functional channel is a dimer of subunits. **B**: TASK-1/3 channels are inhibited by extracellular acidosis.

4. TASK-1 channels in PASMCs

Macroscopic currents that occur due to TASK-1 channels display kinetics and voltage-dependent properties very similar to TASK-3 (i.e. TASK-3 is also an open rectifier) (Kim *et al.*, 2000),(Rajan *et al.*, 2000), but the two channels can be distinguished by the pH range over which their activity is modulated (Fig. 1B). The pK of TASK-1 channels is 7.4, squarely in the physiological range, whereas the pK for TASK-3 channels is shifted to a more acidic level (6.7) (Duprat *et al.*, 1997),(Leonoudakis *et al.*, 1998),(Kim *et al.*, 1998),(Rajan *et al.*, 2000). The TASK-2 channel sequence shares less homology with the other TASK channels and generates outwardly rectifying pH-sensitive currents with a pK of 8.4 (Reyes *et al.*, 1998).

Gurney and colleagues have recently shown the TASK-1 expression in smooth muscle cells of the pulmonary artery in a rabbit (Gurney *et al.*, 2003). The authors have also demonstrated functional expression of a conductance in these cells that is inhibited by extracellular pH, Zn^{2+} and by the endocannabinoid anandamide, but the conductance is insensitive to intracellular Ca^{2+}, 4-aminopyridine and quinine. In addition, the non-inactivating K^+ current is facilitated by halothane causing hyperpolarization of PASMC. These properties closely mimic the pharmacology of heterologously-expressed TASK-1 channels. In order to investigate the expression of TASK channels in human pulmonary arteries we have developed the preparation of primary human pulmonary artery smooth muscle cells. In this study, we demonstrate the expression of TASK-1 mRNAs and proteins in human pulmonary artery smooth muscle cells through the simultaneous absence of TASK-2 and TASK-3 expression (Fig. 6). In addition, we have found an anandamide-sensitive conductance in both primary and cultured human pulmonary artery smooth muscle cells that have properties similar to TASK-1 channels. The native conductance showes an outward rectification in low external K^+ solution, is instantaneous and noninactivating, activated by alkalotic pH, and blocked by anandamide. Transfection of TASK-1 siRNA into human pulmonary artery smooth muscle cells significantly depolarizes the resting membrane potential and abolishes the

effect of pH or anandamide. Respectively, we concluded that TASK-1 channels are responsible for the pH-sensitive, voltage-independent background conductance that sets the resting membrane potential in human pulmonary artery smooth muscle.

5. Role of endothelin-1 in pulmonary hypertension (PH)

Endothelin-1 (ET-1), which is a 21-amino acid peptide that is secreted in the vascular endothelial cells, causes potent and persistent vasoconstriction (Yanagisawa *et al.*, 1988) in vascular tissues. It is important to understand the mechanisms by which ET-1 causes a constriction in the human pulmonary vasculature, since a growing body of evidence implicates ET-1 as an important modulator of the pulmonary vascular tone and suggests ET-1 to be involved in the pathogenesis of pulmonary hypertension. For example, multiple lines of evidences show that ET-1 plays a central role in the pathogenesis of PAH (Hynynen *et al.*, 2006). First, ET-1 is an effective pulmonary vasoconstrictor and induces vascular smooth muscle hyperplasia (Galie *et al.*, 2004). Second, plasma levels of ET-1 are increased in patients with primary and secondary pulmonary hypertension (Galie *et al.*, 2004). Moreover, ET-1 overexpression is associated with PAH (Giaid *et al.*, 1993). Finally, specific pharmacological inhibition of ET-1 receptors attenuates the development of PH (Rubin *et al.*, 2002),(Chen *et al.*, 1995) and prolongs the survival in animal models of PH.

ET-1 has been shown to affect several different types of ion channel in vascular smooth muscles. Various signaling pathways have been implicated in these effects. The binding of ET-1 to G protein–coupled ET_A receptors activates the PLC cascade, thereby initiating the conversion of phosphoinositol to inositol trisphosphate (IP_3) and 1,2-diacylglycerol (DAG), which activates PKC. Once activated, PKC exerts a number of significant effects on vascular smooth muscle cells, including the stimulation of cell proliferation (Zamora *et al.*, 1993) and the modulation of ion channels. Studies have revealed that ET-1 activates receptor-operated Ca^{2+} (Goto *et al.*, 1989),(Inoue *et al.*, 1990), Cl^- (Van Renterghem *et al.*, 1993) and nonselective cation channels (Nakajima *et al.*, 1996),(Oonuma *et al.*, 2000). ET-1 inhibits K_{ATP} channels and K_V channels in coronary and pulmonary arteries, respectively (Miyoshi *et al.*, 1992),(Shimoda *et al.*, 1998),(Shimoda *et al.*, 2001) In addition, Peng et al. (Peng *et al.*, 1998) have demonstrated a dual effect of ET-1 on K_{Ca} currents in cultured human PASMCs, with

ET-1 activating K_{Ca} current at low concentrations and inhibiting K_{Ca} current at high concentrations. Our study demonstrates that ET-1 modulates TASK-1 via the PKC signaling pathway in primary human pulmonary arterial smooth muscle cells.

6. Materials and Methods

6.1 Patch-clamp technique

Erwin Neher and Bert Sakmann developed the patch clamp in the late 1970s (Neher *et al.*, 1976) and early 1980s (Hamill *et al.*, 1981). This discovery made it possible to record the currents of single ion channels for the first time, proving their involvement in fundamental cell processes such as action potential conduction. Neher and Sakmann received the Nobel Prize in Physiology or Medicine in 1991 for their work (Neher, 1992).

6.1.1 Patch clamp

One of the advantages of the patch clamp technique was that it allowed measurements on very small cells such as mammalian cells. The technique can be applied to a wide variety of cells, but was especially useful in the study of excitable cells such as neurons, cardiomyocytes, muscle fibers and pancreatic beta cells. Figure as shown below, the basic principle of this technique was that a fluid filled micropipette containing a silver/silver chloride electrode was brought into contact with the cell membrane. The interior of the pipette was filled with a solution matching the ionic composition of the bath solution. A chlorided silver wire was placed in contact with this solution and conducts electrical current to the amplifier. By applying gentle suction to the pipette, a giga-seal was formed between the pipette and the cell membrane. The high resistance of this seal made it possible to electronically isolate the currents measured across the membrane patch with little competing noise, as well as providing some mechanical stability to the recording. Further suction can rupture the patch of membrane under the tip of the micropipette, providing access for the microelectrode to the interior of the cell; this situation was termed as the whole cell configuration. The whole cell configuration allowed the summed activity of all of the ion channels in the cell membrane (the whole-cell current or macroscopic current) to be measured simultaneously. The investigator can change the composition of this solution or add drugs to study the ion channels under different conditions.

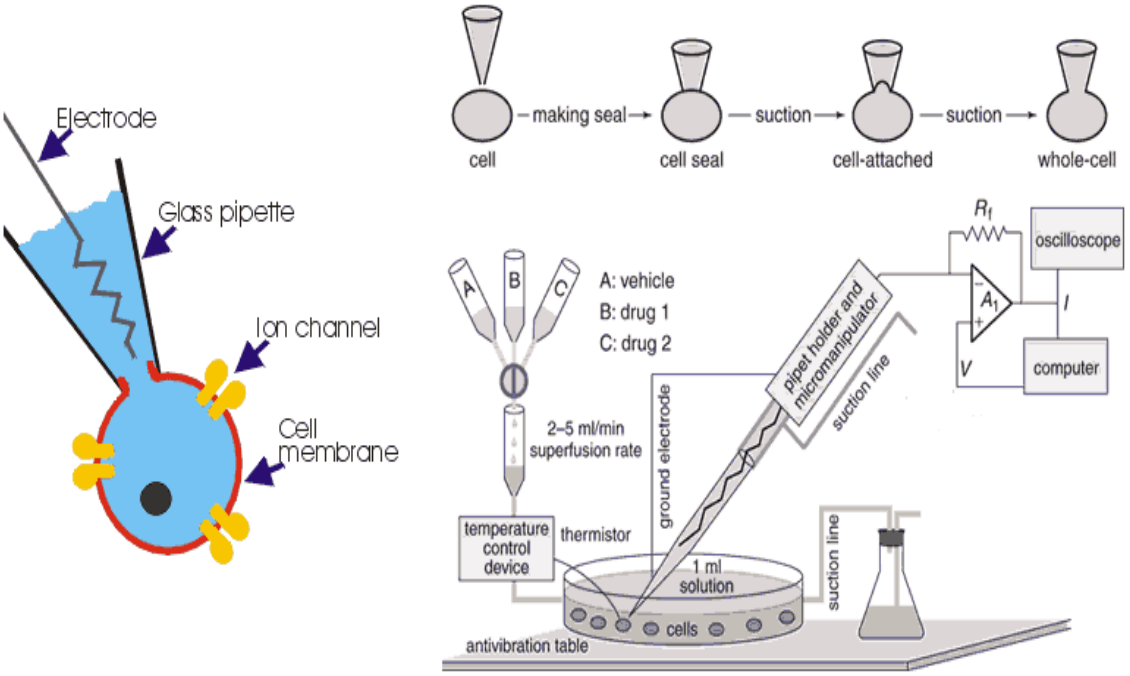

Fig 2: The principle of the whole cell patch-clamp technique (from the online media: http://media.wiley.com/CurrentProtocols/PH/ph1008/ph1008-fig-0002-1-full.gif).

6.1.2 Voltage clamp

The voltage clamp technique allowed the membrane potential of a cell to be clamped at a constant value. The current that flowed through the membrane at any particular potential can be measured. The principle of the technique was to inject a current which was equal in amplitude but opposite in sign to the current flowing across the cell. This results in no net current flowed across the membrane, and the membrane potential remained constant. Therefore, by measuring the current, which had to be injected to clamp the potential, the current flowing across the membrane can be determined. By measuring currents at different clamped membrane potentials it was possible to characterize voltage-gated ion channels.

The principle of this technique is depicted below. The membrane potential amplifier measures membrane voltage and send output to the feedback amplifier. The feedback amplifier subtracts the membrane voltage from the command voltage, which it received from the signal generator. This signal is amplified and returned into the cell via the recording electrode.

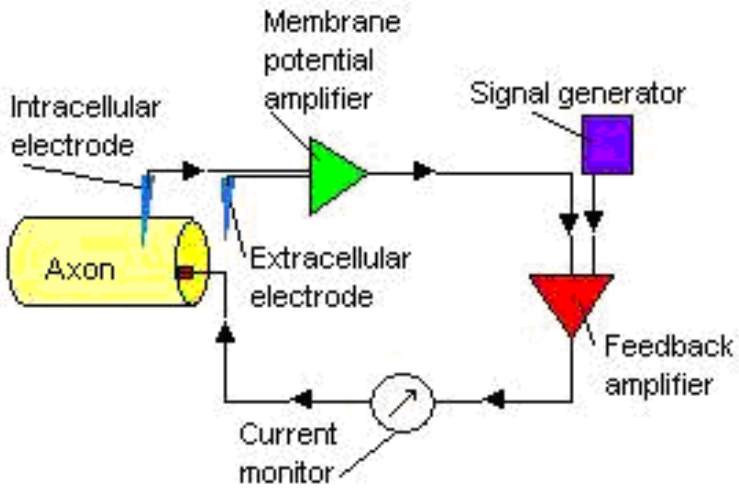

Fig 3: The voltage clamp used a negative feedback mechanism (from the online media: http://wpcontent.answers.com/wikipedia/en/e/ea/Voltage_clamp.jpg).

6.1.3 Current clamp

The basic principle of current clamp is the same as voltage clamp, the only difference is that here current was clamped instead of the voltage. The current clamp technique was used to measure the membrane potential such as the action potential of an excitable cell by injecting current into a cell to keep electrical current constant through the

recording electrode. It can be used for both extracellular and intracellular recordings. Unlike in the voltage clamp mode, where the membrane potential was held at a level determined by the experimenter, in "current clamp" mode the membrane potential was free to vary, and the amplifier recorded whatever voltage the cell generated on its own or as a result of stimulation. This technique was used to study how a cell responds when electric current enters a cell. This was important for instance for understanding how neurons or other excitable cells respond to neurotransmitters and chemical substance that act by opening membrane ion channels.

6.2 Electrophysiology in the present study

The whole-cell patch-clamp technique on hPASMC was used, as previously described, to measure the resting membrane potential under current clamp and macroscopic K^+ currents under voltage clamp (Gurney *et al.*, 2003),(Osipenko *et al.*, 1997),(Hong *et al.*, 2004). Pipette pulled from a borosilicate glass tube (GC 150, Clark Electromedical Instruments, Pangbourne, UK) were fabricated on a model P-97 electrode puller (Sutter Instruments, Novato, CA, USA) and fire polished to give a final resistance of 2 – 3 MΩ for whole-cell recording. A pipette solution filled micropipette containing a silver/silver chloride electrode was gently lowered onto the surface of the cell membrane. By applying gentle suction to the pipette, a giga-seal was formed between the pipette and the cell membrane. Further suction ruptured the patch of the membrane under the tip of the micropipette, providing access for the microelectrode to the interior of the cell; and then the configuration of the whole cell recoding mode was achieved.

To isolate I_{KN} from other voltage-dependent K^+ currents, cells were clamped at 0 mV for at least 5 minutes as described previously (Gurney *et al.*, 2003). The patch-clamp amplifier was Axopatch 200 B (Axon Instruments, Foster City, CA) and the digital-analog converter was DigiData 1320 (Axon Instruments, Foster City, CA) in all voltage- and current-clamp experiments. Offset potentials were nulled directly before formation of a seal. No leak subtraction was made. Cells expressing holding current at -70 mV of 10

pA before or during the recordings were discarded. Estimation of cell capacitance (in pF) was made from whole-cell capacitance compensation. For resting membrane potential, cells were held in current-clamp at their resting Em (without current injection). The effective corner frequency of the low-pass filter was 0.5-5 kHz. The frequency of digitization was at least twice that of the filter. The data were stored and analyzed with commercially available pCLAMP 9.0 software (Axon Instruments, Foster City, CA, USA).

6.3 Preparation of human pulmonary artery smooth muscle cells

The primary human pulmonary artery smooth muscle cells (PASMC) for this study were either purchased from Lonza (Lonza Group Ltd, Switzerland) and maintained according to the manufacturer's instructions or isolated from human pulmonary arteries of lung cancer patients (n = 39) undergoing lung surgery without a history of pulmonary vascular disease or arterial hypoxemia. The study protocol for tissue donation was approved by the “Institutional Review Board” of the Justus-Liebig-University Gießen and the Medical University of Graz in accordance with the national law and with the guidelines on Good Clinical Practice/International Conference on Harmonization. Written informed consent was obtained from each individual patient.

A

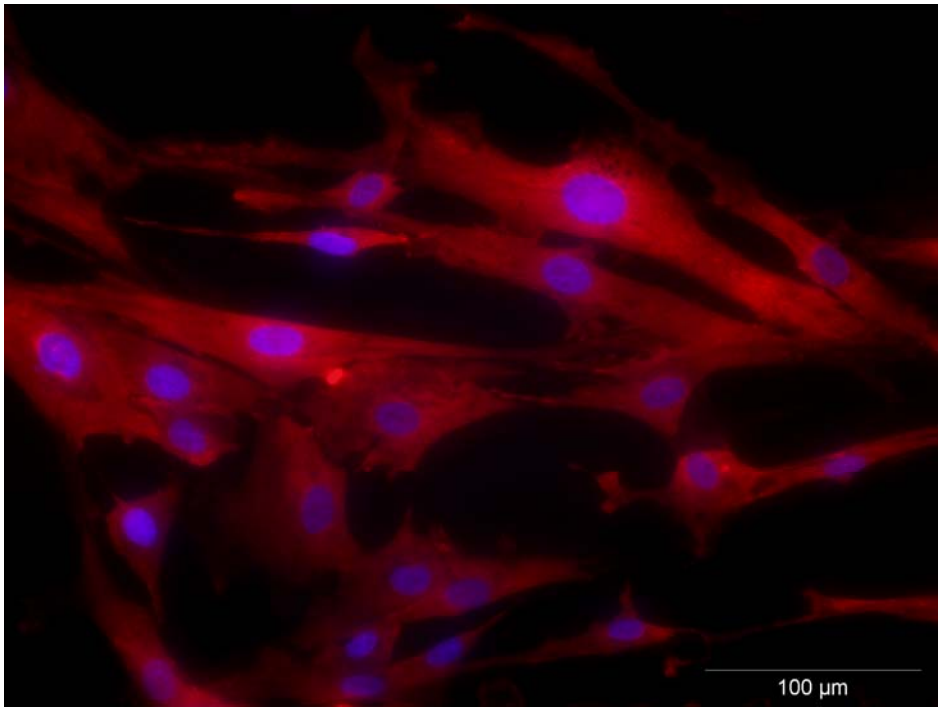

B

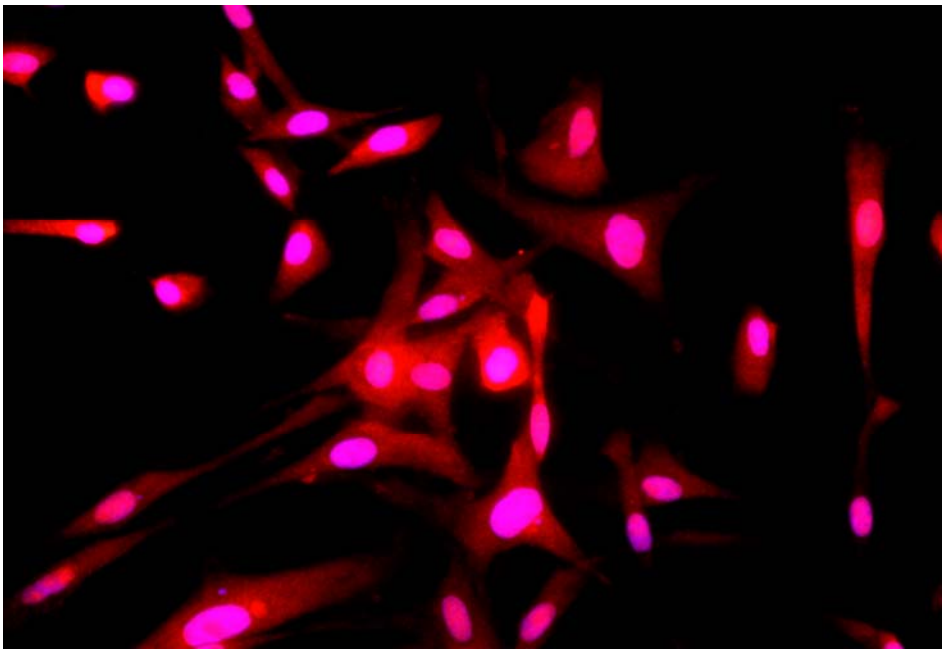

Fig 4: Immunofluorescence staining for smooth muscle cell

At least 95% of cells alpha-actin (**A**) and myosin heavy chain-7 (**B**) stained positive in human pulmonary smooth muscle cells.

Preparation procedure of the primary human PASMCs: The adventitia of small arteries with diameters of <1 mm was carefully removed under microscopic guidance and media pieces <1 mm^3 were placed on 16-mm coverslips with 500 µl culture medium (Lonza SMC Medium; Lonza Group Ltd, Switzerland). Cells were maintained at 37 °C. Medium was initially changed after 24 h and every 48 h thereafter. PASMCs grown on coverslips were used for patch-clamp recordings within 6 days. Cells were sub-cultured in Petri dishes to 70 – 90 % confluent at passages 3–6 for molecular biology studies. SMC identity was verified by their characteristic appearance in the phase-contrast microscopy. The purity of the PASMC cultures was confirmed using indirect immunofluorescent antibody staining for smooth muscle-specific isoforms of α-actin and myosin heavy chain-7(at least 95% of cells stained positive. Fig. 4), and lack of staining for von Willebrand factor.

6.4 Solutions and chemicals

All compounds were purchased from Sigma Chemical Company (St. Louis, MO). Stock solutions of U-73122, OAG, R59949, Rottlerin, Gö6983 and KT5720 were prepared in DMSO and methanol separately. In addition, anandamide was dissolved in 50 (v/v)% ethanol in water. Application of the vehicle used in the study alone at a maximal concentration (1:1,000 dilution of DMSO, ethanol or methanol in Ringer bath solution) had no effect on K^+ current or resting membrane potential. The pH of solutions containing drugs was tested and corrected to eliminate potential pH-induced effects. They were diluted with bath solution to the appropriate concentration on the day of the experiment.

The interior of the pipette was filled with pipette solution (Table 1); pH has been adjusted to 7.2 with KOH. The pipette solution with K-methanesulphonate was to suppress Cl^- currents. The free $[Ca^{2+}]$, calculated using Maxchelator (http://www.stanford.edu/%7Ecpatton/maxc.html), was 30 nM. Cells were superfused at room temperature with bath solution-1 (Table 2); then the pH has been adjusted to pH 7.3 with NaOH. When High-K^+ - bath solution (bath solution-2) was applied, then the pH has been adjusted to pH 7.3 with NaOH. The hypoxic bath solution was bubbled with N_2. This procedure produced pO_2 values in the cell chamber of 24–30 mmHg under hypoxic conditions (ABL TM510, Radiometer, Copenhagen, Denmark), pH was 7.40.
The isolated mouse lung was perfused with Krebs Henseleit buffer as shown below (Table 3), then the pH has been adjusted to 7.37 - 7.40 with $NaHCO_3$.

Solutions used for the study are listed below.

Table 1: Pipette solution

(All concentration in mmol/L)

	KCl	K-methanesulphonate	$MgCl_2$	Na_2ATP	EGTA	HEPES
Composition	20	135	1	2	3	20

Table 2: Bath Solution

(All concentration in mmol/L)

	NaCl	KCl	$CaCl_2$	$MgCl_2$	glucose	Na_2HPO_4	KH_2PO_4	HEPES
Solution-1	140.5	5.5	1.5	1	10	0.5	0.5	10
Solution-2	10	155	1.5	1	10	0.5	0.5	1

Table 3: Krebs Henseleit buffer

(All concentration in mmole/L except hydroxyethylamylopectin)

	NaCl	KCl	KH_2PO_4	$CaCl_2$	$MgCl_2$	glucose	Hydroxyethylamylopectin
	120	4.3	1.1	2.4	1.3	13.32	5% [wt/vol]

6.5 Relative mRNA quantification

Real-time PCR was used for the relative quantitation of the TASK-1, TASK-2, TASK-3, PRKCA, and PRKCE mRNA. Both, GAPDH and HMBS, were used as reference genes (as shown in table 4). The primers were designed to be intron-spanning where possible and maximal specific for the target genes. The reactions were performed in an ABI 7700 Sequence Detection System (Applied Biosystems, Foster City, CA) using SYBR-Green I as fluorogenic probe in 25 µl reactions containing 2 µl cDNA sample, 1× qPCR^{TM} Mastermix for SYBR Green I (Eurogentec, Seraing, Belgium), 45 pmol forward and reverse primer (Table 4). The cycling protocol was 1× (50 °C, 2 min); 1× (95°C, 6 min); 45× (95 °C, 5 s; 60 °C, 5 s, 73 °C, 10 s). Data for the amplification curves were acquired after the extension phase at 73 °C. After amplification, a melting curve was recorded and analyzed in order to identify possible contributions of unspecific products to the fluorescence signal. Additionally, an agarose-gel analysis was performed to confirm the primary formation of a single specific PCR product. The background signal of the amplification curves was individually corrected for each gene using the signals recorded from cycle 3 to cycle 15-25, depending on the onset of the exponential signal increase. The threshold value for each gene was set in the middle of the overlapping region of the exponential phases. Each gene was measured in duplicate in two independent experiments. The Δct values for each target gene were calculated for both reference genes using the averaged ct values by the formula $\Delta ct = ct_{target} - ct_{reference}$. The Δct of both reference genes were averaged and used to calculate the ΔΔct value by $\Delta\Delta ct = \Delta ct_{siRNA} - \Delta ct_{control}$. According to an amplification efficiency of approximately 2, the factors of differential target expression were calculated by $f = 2^{-\Delta\Delta ct}$ (the efficiencies for the amplification of the target genes were determined in pilot experiments and were all greater than 1.98 or 98%, respectively; data not shown). The error of the ΔΔct values was estimated from the average standard deviation of replicates using the error propagation by Gauss.

Table 4:

Primers used for quantitative real-time PCR

Target Gene	Genbank Accsession	Sequence 5'→3'	Length (nt)	Exon[1]	Pos[2]	Amplicon Length (bp)
TASK-1	NM_002246	CGGCAAGGTGTTCTGCATG	19	2	440	91
		CAAGGTGTTGATGCGCTCG	19	2	512	
TASK-2	NM_003740	CCTTCATCACCATCTCCACCA	21	4	929	94
		TCCACGAAGTAGCGGTACAGG	21	5	1002	
TASK-3	NM_016601	GATGAAACGCCGGAAGTCC	19	2	1165	104
		AAATCCCGAAGCCGTGTTC	19	3	1250	
PRKCA	NM_002737	GATGGATGGAGTCACGACCAG	21	13	1511	114
		AGGACGCCATAGGCCCA	17	14	1608	
PRKCE	NM_005400	CGGAAACACCCGTACCTTACC	21	10	1587	139
		GTGAACGAGGCTCGTCGAA	19	11	1707	
GAPDH	NM_002046	CGTCATGGGTGTGAACCATG	20	6	468	81
		GCTAAGCAGTTGGTGGTGCAG	21	7	528	
HMBS (PBGD)	NM_000190.2	TGTCTGGTAACGGCAATGCG	20	1	153	70
		CCCACGCGAATCACTCTCAT	20	3	203	

[1] Number of the exon in which the primer sequence is located.

[2] Position of the 5' nucleotide of the primer relative to the Genbank sequence.

6.6 Design and transfection of siRNA for human TASK-1

The target sequence of siRNA was localized 261 bases downstream from the start codon of human TASK-1 (GenBank accession no. AF006823). The forward and reverse strands (UCA CCG UCA UCA CCA CCA U dTdT) and (AGU GGC AGU AGU GGU GGU A dTdT) with two 5' deoxy-thymidine overhangs were commercially synthesized (Eurogentec, Seraing, Belgium) and annealed at a final concentration of 20 µmol/L each by heating at 95 °C for 1 minute and incubating at 37°C for 1 hour in annealing buffer (20 mmol/L Na-acetate, 6 mmol/L HEPES–KOH [pH 7.4], and 0.4 mmol/L Mg–acetate). Transfection of siRNA was performed at a final concentration of 40 nmol/L using Oligofectamin (Invitrogen). As a control, a random siRNA sequence (siRNA-ran: UAC ACC GUU AGC AGA CAC C dTdt) prepared as described above was used. RNA and electrophysiological measurements were performed 48 to 72 hours after siRNAs transfection. For assessment of the transfection efficiency, a fluorescein isothiocyanate (FITC)-conjugated siRNA (QIAGEN) was used. The intracellular localization was assessed by direct visualization of the FITC by fluorescence microscopy after transfection.

6.7 Immunoprecipitation

Cultured smooth muscle cells were solubilized as previously described (Vadasz *et al.*, 2005) in an extraction buffer supplemented with 1 mmol/L sodium orthovanadate, 10 mmol/L sodium pyrophosphate, 5 mmol/L β-glycerophosphate, and 50 mmol/L sodium fluoride. The TASK-1 was immunoprecipitated from cell lysates (4 hours; 4 °C) using rabbit anti–TASK-1 (Alomone Labs, Jerusalem, Israel)(Hsu *et al.*, 2004). Antibodies were chemically coupled to protein A–Sepharose beads using a Seize Immunoprecipitation Kit (Pierce, Rockford, Ill). Immunoprecipitates were washed to a final stringency of 470 mmol/L NaCl in extraction buffer. Immunoprecipitates were

resolved on a 10% Tris–Tricine SDS-PAGE gel, and blots were probed with rabbit anti–TASK-1 (1:500; Alomone Labs), mouse anti-phosphotyrosine (1:1750; Cell Signaling Technologies, Beverly, Mass), or mouse anti-phospho(Ser/Thr) (1:1000; Cell Signaling Technologies) antibodies, respectively.

6.8 Immunofluorescence staining

Immunofluorescence, as previously described, was performed using two different antibodies directed against unique domains of TASK-1, one at the amino terminus (Santa Cruz Biotechnology) and the other between residues 252 and 269 of the protein's carboxyl terminus (Alomone Labs)(Gurney *et al.*, 2003). hPASMCs grown on glass slides were fixed for 5 minutes in cold methanol, rinsed 5 times in PBS. After blocking with 1% BSA overnight, cells were incubated with anti-TASK-1 antibody (1:50 dilution) for 1 hour then probed for 40 minutes with fluorescent labelled secondary antibodies (anti-goat IgG-FITC or anti-rabbit Alexa 555). Cells were counterstained with DAPI to identify the nuclear DNA. Duplicates were processed without primary antibodies as controls. Fluorescence was imaged with a Leica DM2500 M microscope, using Leica 40x (N.A. 1.0) objective.

6.9 Isolated, perfused and ventilated mouse lungs

All organ experiments were approved by the local authorities. Lungs from C57BL/6 mice (Charles River, Germany) were removed from the chest in deep anaesthesia (Weissmann *et al.*, 2006) (pentobarbital sodium; 100 mg/kg body weight) while being perfused with Krebs Henseleit buffer (Table 3). The total system volume was 15 ml, the buffer flow rate was 2 ml/min, and left atrial pressure was set at 1.5 - 2.0 mm Hg. The isolated lungs were ventilated with a gas containing 5.3 % CO_2, 21.0 % O_2, balanced with N_2 (positive pressure ventilation with a tidal volume of 300 µl, 90 breath/min, and 3 cmH_2O positive end-expiratory pressure). The isolated lungs were freely suspended from a force transducer for continuous monitoring of organ weight. The whole system was heated to 37° C. Pressures in the pulmonary artery, the left atrium and the trachea were continuously registered. Lungs included in the study were those that had a homogeneous white appearance with no signs of hemostasis, edema or atelectasis. After an initial steady state period of 30 min, ET-1 was added in to the buffer in increasing doses every 25 min. In experiments with anandamide this agent was applied to the buffer 20 min prior to the first ET-1 admixture. Delta PAP indicates the pulmonary arterial pressure after application of ET-1 at a chosen concentration minus the pulmonary arterial pressure before.

Fig 5. **Scheme of the isolated perfused mouse lung.**

The perfusion system is drawn in black, the ventilation system in gray. Water circulation system is marked by black waves. From (von Bethmann *et al.*, 1998)

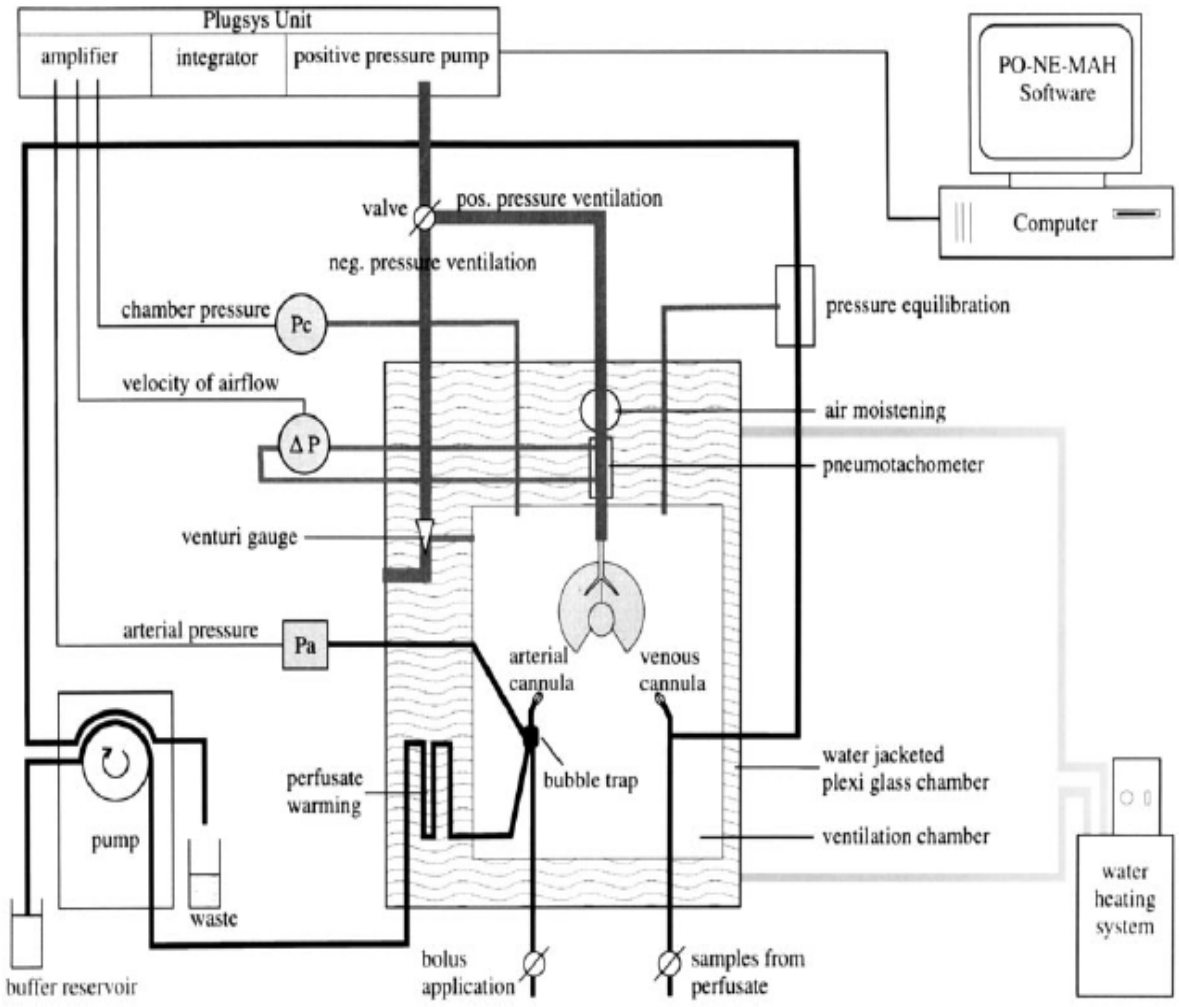

6.10 Statistical analysis

Numerical values are given as means ± SE of n cells. Intergroup differences were assessed by a factorial analysis of variance with post hoc analysis with Fisher's least-significant difference test or Student's unpaired and paired *t* tests as appropriate. Probability values of <0.05 were considered significant. The mean data at different anandamide concentrations were fitted.

To determine the blocking potency of endothelin-1 on TASK-1, concentration–inhibition curves were constructed from the current inhibition by the drug at 0 mV. I/I_0 is the current in the presence of ET-1 as a fraction of the current before ET-1 application. The normalized amplitudes of currents were fitted by means of a nonlinear least-squares method with the best-fit Hill equation: $E=E_{max}/(1+(IC_{50}/c)^h)$, where E is the percentage for inhibiting I_{KN} at a concentration c of the drug concentration, E_{max} was the maximum effect, IC_{50} was the concentration giving a half-maximum effect and h was the Hill coefficient. Because the Hill coefficient was less than 1 (0.9 in all curves), it was set to one, accounting for a 1:1 binding stoichiometry.

7. Results

7.1 Characteristics of K_{2P} channel in hPASMC

7.1.1 Expression of TASK-1 channels

The TASK-1 protein in hPASMC was established with two TASK-1 antibodies, anti-rabbit Alexa 555 antibodies or anti-goat IgG-FITC antibodies, directed against the carboxyl or amino terminal region of the protein, respectively (n=4; Figure 6A and 6B). In contrast, staining was absent in control cells treated in the same way but without an exposure to a TASK-1 antibody (Figure 6C and 6D). PCR studies demonstrated the presence of TASK-1, TASK-2, and TASK-3 in human brain tissue, but only TASK-1 mRNA was detected in primary and in cultured hPASMC as well (Figure 6E).

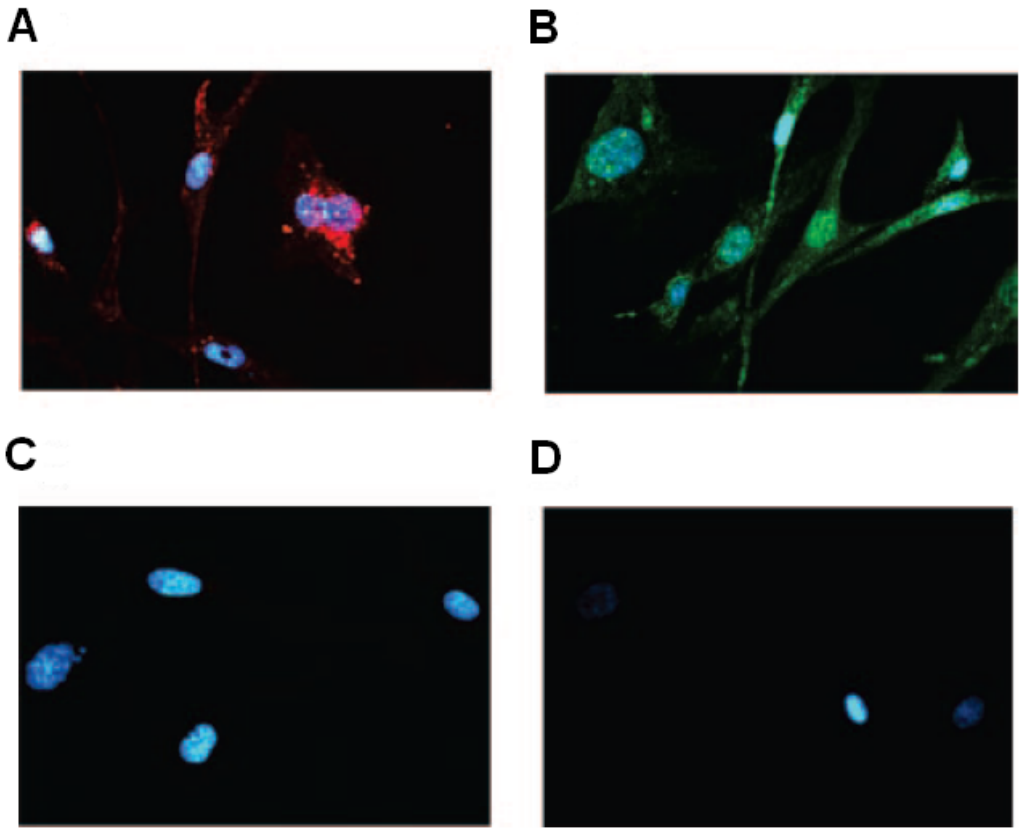

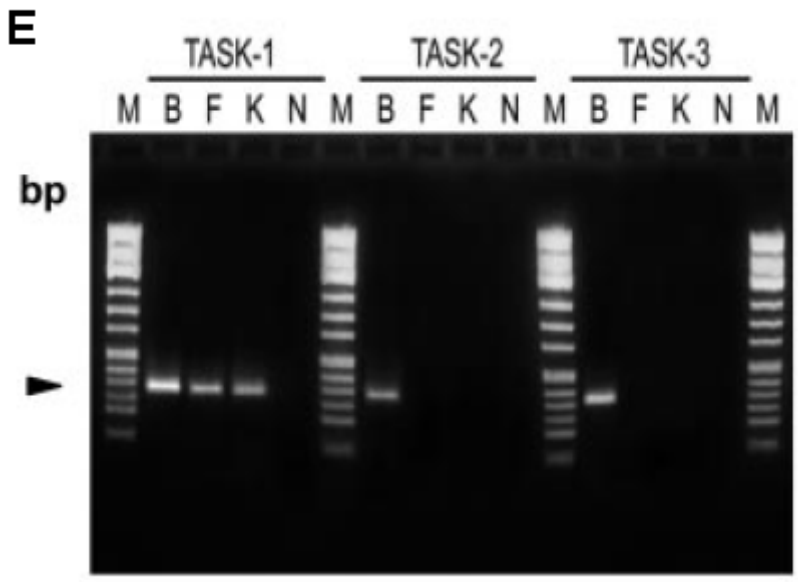

Fig 6. TASK-1 expression in hPASMC. (from Olschewski *et al.*, 2006)

Fluorescence images of hPASMC stained with the Alomone C-terminal TASK-1 with anti-rabbit Alexa 555 antibodies (**A**) or the Santa Cruz N-terminal TASK-1 with anti-goat IgG-FITC antibodies (**B**). Staining was absent in control cells treated identically but without an exposure to the primary antibody, as shown by matched fluorescence (**C** and **D**, respectively). **(E)** The Representative gel shows mRNA expression of TASK-1 (91 bp), TASK-2 (94 bp), and TASK-3 (104 bp) in human brain tissue (B), primary hPASMC (F), and cultured hPASMC (K). Only TASK-1 is expressed in primary and cultured hPASMC. The arrow indicates 100 bp: M, the molecular weight marker used to indicate the size of the PCR fragments: N, no template control. Identical results were obtained with at least 3 additional preparations of RNA.

7.1.2 The pharmacological properties of TASK-1 channels

Anandamide, a member of the endogenous cannabinoids, has been recently shown to be a direct and selective blocker of the TASK-1 channels (Gurney *et al.*, 2003),(Maingret *et al.*, 2001). As depicted in Figure 7, the application of 10 µmol/L anandamide markedly but reversibly inhibited the noninactivating K^+ current (I_{KN}) in primary hPASMC from 16 ±2 pA to 6±2 pA (P<0.05), recorded at 0 mV after the cells were clamped at 0 mV for at least 5 minutes to inactivate voltage-dependent K^+ channels. Figure 7A showed a representative recording from the holding potential of 0 mV; the voltage was stepped to 60 mV and then ramped to -100 mV over a period of 1.6 seconds. The current during the ramp reflects I_{KN} parallel with a nonspecific “leak” current and reverses direction at the resting potential of the hPASMC (Gurney *et al.*, 2003),(Osipenko *et al.*, 1997). As a consequence of the inhibition of the outward current, anandamide also influenced the reversal potential of the current (Figure 7A). The “difference” current, obtained by subtracting the current remaining in the presence of anandamide from that obtained under control conditions (Figure 7B, inset), was reversed close to -84 mV, the calculated Nernst equilibrium potential for K^+ under these conditions. Maintenance of a resting membrane potential in rabbit PASMC had been proposed to involve TASK-1(Gurney *et al.*, 2003). Indeed, anandamide significantly depolarized hPASMC (9±1 mV; n=5; P<0.05). Under symmetrical K^+ conditions in the same cell, anandamide caused a marked inhibition of the K^+ current (Figure 7B). The difference current (inset) was linear and reversed at or near 0 mV, the calculated Nernst equilibrium potential for K^+ under these conditions. This pharmacological and biophysical profile demonstrated the functional expression of the K^+-selective background channel TASK-1 in primary hPASMC.

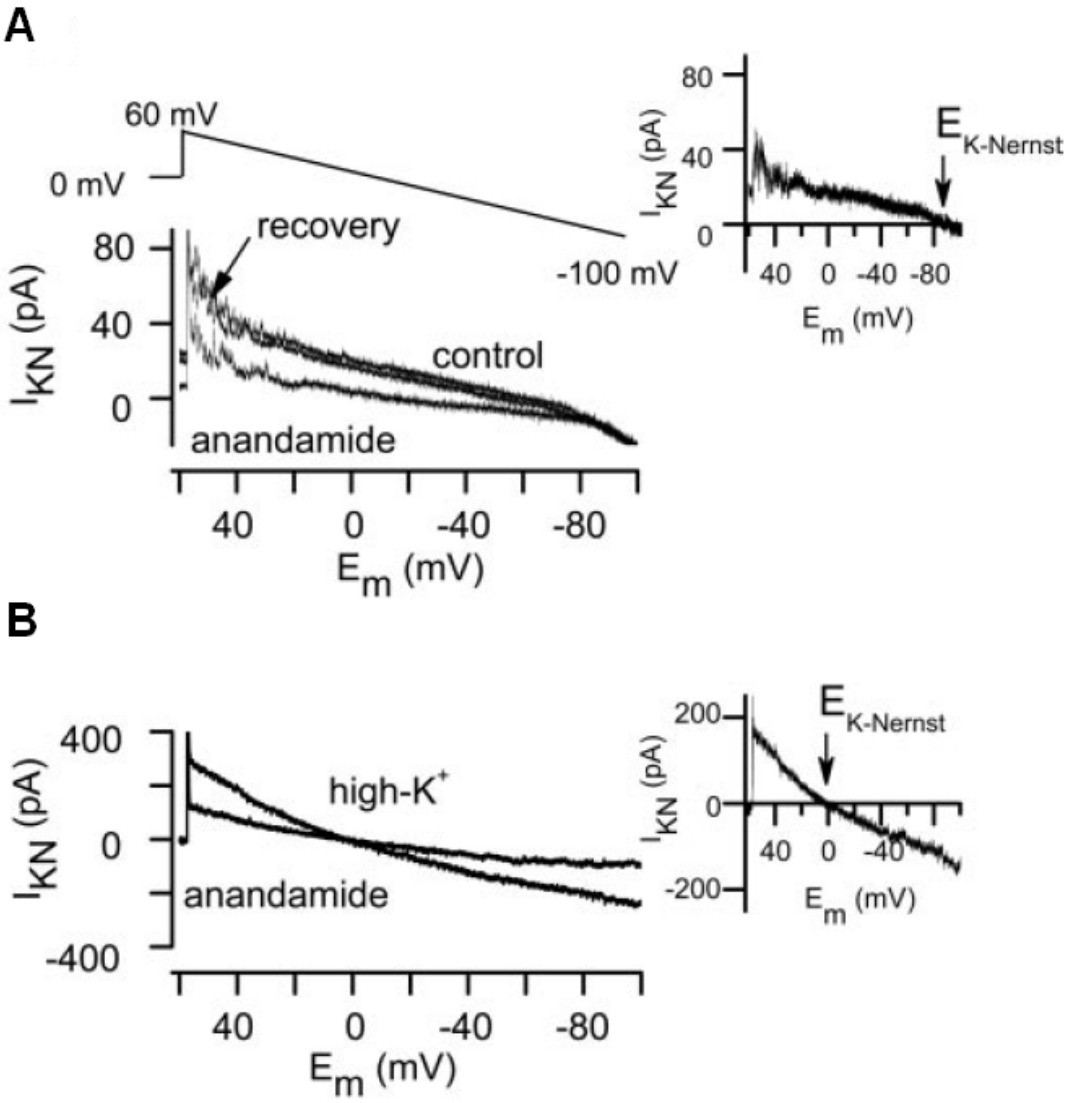

Fig 7: I_{KN} in human PASMC (from Olschewski *et al.*, 2006; recordings performed by Bi Tang and Yingji Li)

(**A**) Effect of 10 µmol/L anandamide on I_{KN} recorded during ramp, voltage protocol inset (left) and difference current trace, obtained by subtracting current amplitudes in the presence of TASK-1 blocker from those obtained under control conditions (right). Difference current reversed close to -84 mV, as expected for a K^+-selective conductance under these conditions. (**B**) I_{KN} evoked under symmetrical (155 mmol/L K^+) conditions by ramp in the same cell (voltage protocol above), before (high-K^+) and during the application of 10 µmol/L anandamide (left) and trace of difference currents (right). Difference current was voltage independent and reversed close to 0 mV, as expected for a K^+-selective conductance under these conditions.

The essential property of the TASK-1 channels is their extreme sensitivity to variations in extracellular pH (pHo) in a narrow physiological range. Figure 8A shows the pHo dependence of I_{KN} of primary hPASMC across the full voltage range over which I_{KN} is apparent. Modification of I_{KN} by pHo was reflected in the resting membrane potential. A pH of 8.3 significantly hyperpolarized the cells, whereas acidification caused membrane depolarization in primary hPASMC (-10±1 mV versus 13±2 mV; n=5). Overall, we have found a functional expression of kinetically and pharmacologically identical background K^+ current carried by TASK-1 in primary hPASMC. In order to provide a certain evidence for the involvement of TASK-1 in I_{KN}, we tested the effects of 10 mmol/L tetraethylammonium (TEA, a blocker of K_{Ca}), 3 mmol/L 4-aminopyridine (4-AP, a blocker of K_V), 5 µmol/L ruthenium red (a blocker of TASK-3), and different concentrations of $ZnCl_2$. We found that TEA and 4-AP failed to inhibit I_{KN} (Figure 8B). In contrast, ruthenium red caused a reduction of I_{KN} (Figure 8C). However, the ruthenium red–sensitive current was linear and the reversal potential varied between 0 and -20 mV. The calculated Nernst equilibrium potential was -84 mV for K^+. It is well known that the ruthenium red is active at various sites (eg, ryanodine receptors (Hohenegger *et al.*, 2002) and TRPV channels (Guler *et al.*, 2002), therefore, this effect in primary hPASMC was not be surprising. The divalent zinc cation was also reported to inhibit TASK-1 at higher concentrations. However, in our study, the Zn-sensitive ion current had a reversal potential close to 0 mV (Figure 8D), indicating the presence of a nonspecific leak current.

Both, the potency of anandamide and pH 6.3 for blocking I_{KN}, and pH 8.3 for activating it, together with their effects on measured resting membrane potential (*E*m), strongly suggest that I_{KN} maintains the resting membrane potential in primary hPASMC.

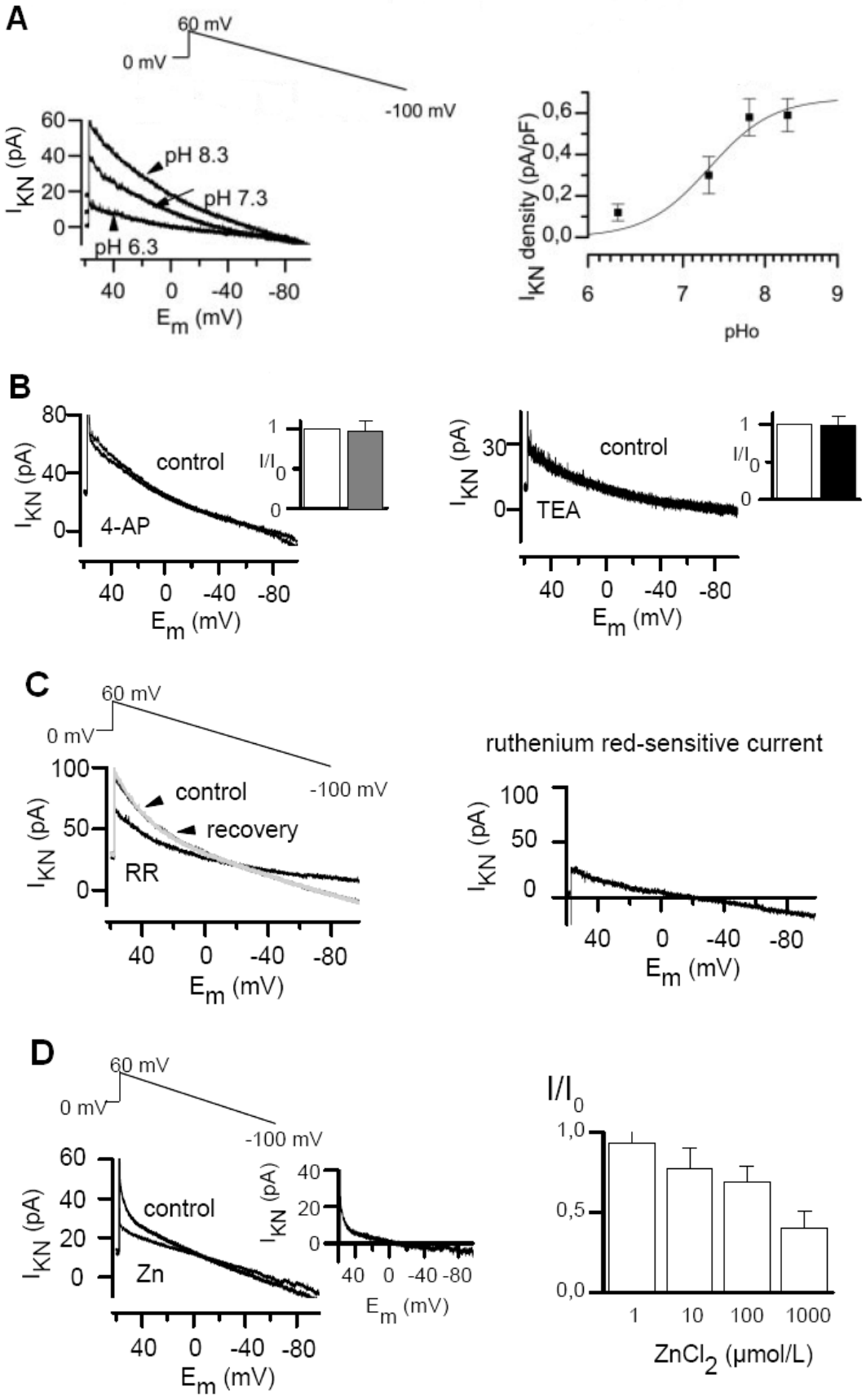

Fig 8. Characterization of I_{KN} in hPASMC (from Olschewski *et al.*, 2006)

(**A**) Representative time-course plot of I_{KN} at different pHo in primary hPASMC recorded

by ramp, activated from a holding potential of 0 mV during 1.6 second from 60 to -100 mV(left). Relationship between pH_o and I_{KN} measured at 0 mV (right). Data were fitted with a Boltzmann relationship with $pH_{0.5}$ 7.3 for primary hPASMC. (**B**)TEA (10 mmol/L) and 4-AP (3 mmol/L) failed to inhibit I_{KN}. (**C**) Effect of ruthenium red on I_{KN} recorded during ramp in primary hPASMC (left), and "difference" currents trace, obtained by subtracting the current amplitudes in the presence of ruthenium red from those obtained under control conditions (right). Difference current reversed close to 0 mV. (**D**) Effect of $ZnCl_2$ on I_{KN} in hPASMC recorded during ramp, and "difference" currents trace (insert). Difference current reversed closed to 0 mV. The histogram summarized the effect of different concentrations of $ZnCl_2$ on I_{KN} calculated at 0 mV in cultured hPASMC (n = 4 each group). I/I_0 is the current in the presence of $ZnCl_2$ expressed as a fraction of the current prior to the $ZnCl_2$ application.

7.1.3 The Effects of TASK-1 knockdown in hPASMC

In order to further confirm the role of the TASK-1 channels in the regulation of Em in hPASMC, we knocked down the TASK-1 expression in the cells via TASK-1 siRNA. Electrophysiological measurements were performed 24 to 48 hours after transfection of siRNAs. We found that the TASK-1 siRNA efficiently suppressed TASK-1 mRNA levels without affecting other widespread enzyme systems such as protein kinase C (PKC) (Figure 9A). The knockdown of TASK-1 caused a depolarization of the resting membrane potential compared to the control cells (-26±1 mV versus -40±2 mV; $P<0.05$; Figure 9B). As shown in Figure 9C, pretreatment of hPASMC with TASK-1 siRNA inhibited the suppression of I_{KN} by anandamide or acidosis (from 3±1 pA to 2±1 pA, from 3±1 pA to 3±1 pA, respectively). There was no significant activation of alkalosis (from 4±1 pA to 3±1 pA). However, I_{KN} was demonstrated to be inhibited by acidosis or anandamide, and activated by alkalosis in hPASMC transfected with scrambled sequence TASK-1 siRNA (Figure 9D and 9E). Therefore, these results strongly suggest that TASK-1 is a major contributor to I_{KN}, and further confirm the role of the TASK-1 channels in the regulation of Em in hPASMC.

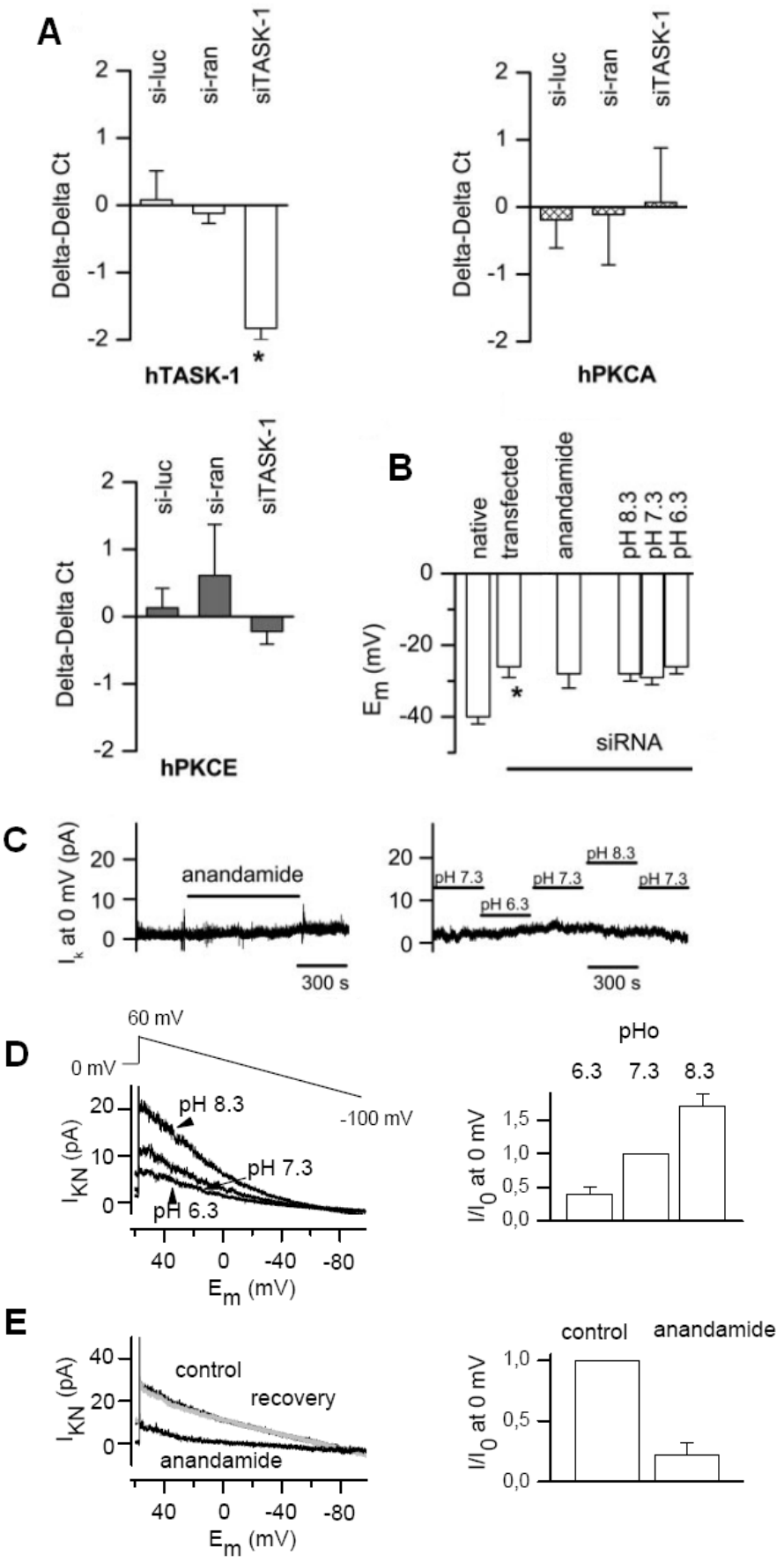

Fig 9. Effects of TASK-1 knockdown on hPASMC (from Olschewski *et al.*, 2006; recordings performed by Bi Tang and Yingji Li)

(**A**) Regulation of human TASK-1 (hTASK-1), human PKCα (hPKCA), and human PKCε (hPKCE) as measured by real-time RT-PCR (**P*<0.05, 1-sample *t* test with H_0: ΔΔCt=0). The ΔΔCt values are calculated as described in chapter 6. Positive values indicate an upregulation of the target gene compared to controls; negative values a downregulation. The ΔΔCt values are approximately proportional to the binary logarithm of the fold change. (**B**) Resting membrane potential of native control, and transfected cells shown left (**P*<0.01). The E_m is significantly depolarized in transfected cells. Lack of changes in E_m under anandamide or pH_o in transfected cells (n=5 each group). (**C**) Effect of 10 µmol/L anandamide and pH_o on remaining I_{KN} recorded at 0 mV. Effect of pH_o (**D**) and 10 µmol/L anandamide (**E**) on remaining noninactivating current (I_{KN}) recorded at 0 mV in hPASMC transfected with scrambled sequence TASK-1 siRNA.

7.1.4 Acute hypoxia inhibits TASK-1

Due to previous work that implicated the TASK-1 channel as an important molecular component of the O_2-sensitive K^+ current in PASMC (Gurney *et al.*, 2006), we investigated the O_2 sensitivity of this channel in primary hPASMC. Representative traces recorded by ramp, before and after five minutes of exposure to hypoxic solutions, are shown in Figure 10A. The hypoxia-sensitive current reversed close to -84 mV. Consistent with the involvement of the TASK-1 channels in this inhibition, the current was not further blocked through anandamide (Figure 10A, bottom panel). Under current-clamp conditions, hypoxia caused a marked cell depolarization (by 10±1 mV; n=9; $P < 0.05$). Pretreatment of hPASMC with TASK-1 siRNA inhibited significant suppression of I_{KN} by hypoxia (Figure 10B). Figure 10C summarizes the mean data confirming that hypoxia significantly inhibited TASK-1 in primary hPASMC.

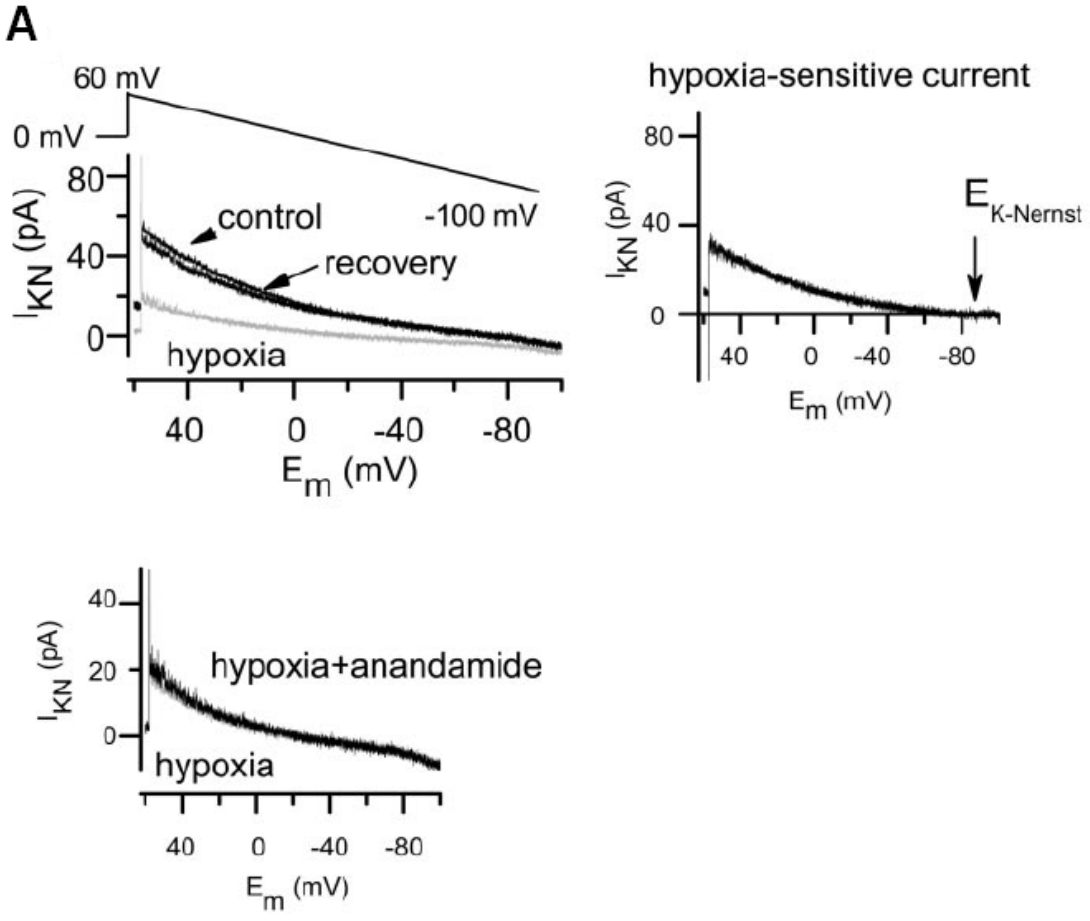

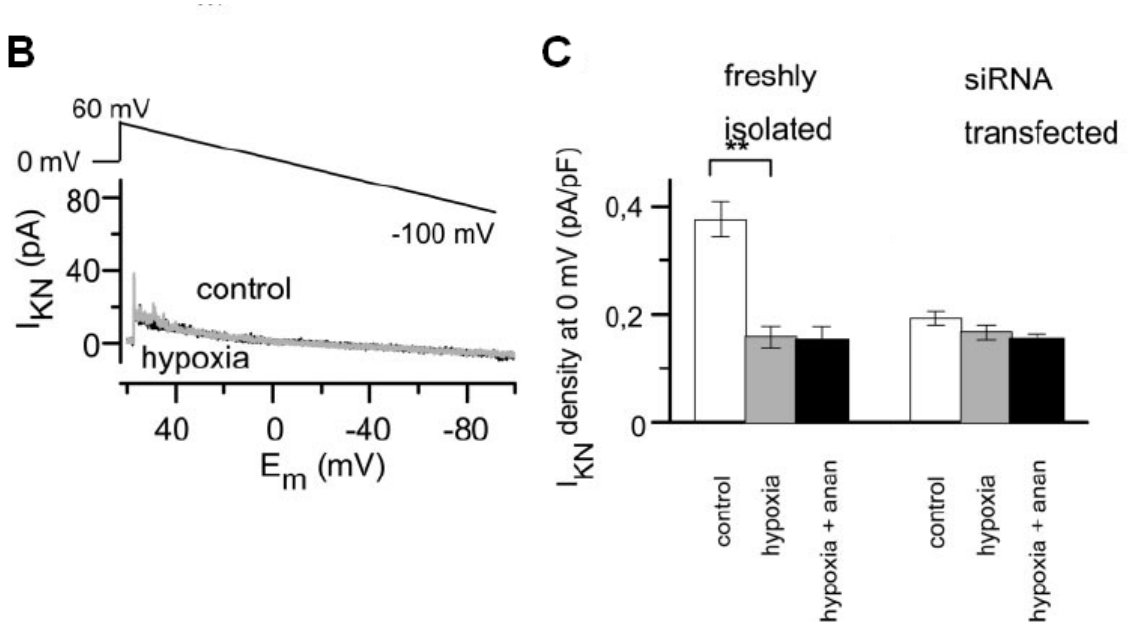

Fig 10. Hypoxia blocks TASK-1 in hPASMC (from Olschewski *et al.*, 2006)

(**A**) Effect of hypoxia on I_{KN} recorded by ramp in primary hPASMC (left) and difference currents trace, obtained by subtracting the current amplitudes in the presence of hypoxia from those obtained under control conditions (right). Difference current reversed close to -84 mV, as expected for a K^+-selective conductance under these conditions. $E_{K\text{-}Nernst}$ indicates Nernst equilibrium potential. Application of 10 µmol/L anandamide under hypoxic conditions did not cause a further change in the current (bottom), suggesting that the hypoxia-sensitive current is carried by TASK-1. (**B**) Lack of hypoxia effect on I_{KN} in siRNA-transfected hPASMC. (**C**) The histogram summarizes the effect of hypoxia and anandamide (anan) under hypoxic conditions on I_{KN} calculated at 0 mV in primary and siRNA-transfected hPASMC (n=5 each group; $^{**}P<0.01$).

7.2 Modulation of TASK-1 by endothelin-1 in hPASMC

7.2.1 Endothelin-1 inhibits TASK-1

As shown in figure 11A, ET-1 significantly and dose-dependently depolarized hPASMCs. Application of ET-1 markedly reduced the non-inactivating K^+ current in primary hPASMCs in the presence of the voltage-gated K^+ channel inhibitor 4-aminopyridine (4-AP) (5 mM, data not shown). Figure 11B shows the effect of ET-1 in representative recordings from the holding potential of 0 mV, after the cells were clamped at 0 mV for at least 5 min to inactivate the voltage-dependent K^+ channels. The voltage was stepped to 60 mV and then ramped to -100 mV over a period of 1.6 seconds. The ET-1-sensitive current, obtained by subtracting the current remaining in the presence of ET-1 from that obtained under control conditions (Figure 11B insert), was reversed close to -84 mV, the calculated Nernst equilibrium potential for K^+ under these conditions. The effect of ET-1 on I_{KN} was completely abolished by pre-application of 10 µM anandamide (Figure 11C), a TASK channels blocker (Gurney *et al.*, 2003), (Maingret *et al.*, 2001). Due to our data showing that TASK-2 and TASK-3 are not expressed in hPASMC, this finding suggests that ET-1 acts on the TASK-1 current. Another property of TASK channels is their sensitivity to extracellular pH and to volatile anesthetics. As illustrated in Figure 11E (left), the ET-1 inhibited current was not further reduced by acidosis (pH 6.3). Consistently, reducing the pH from 7.3 to 6.3 suppressed I_{KN}. Under this acidification, ET-1 did not further inhibit the current (Figure 11E, right). Application of isoflurane, well known activator for TASK-1, (1mM) enhanced I_{KN} (Figure 11F). Consistent with the involvement of the TASK-1 channels in this facilitation, I_{KN} was blocked by ET-1. The concentration-response curve for TASK-1 inhibition by ET-1 measured and calculated at 0 mV resulted in an IC_{50} of 1.6 ± 0.3 nM (Figure 11D; n = 5 for each group).

In order to further confirm the role of TASK-1 in the ET-1 pathway in hPASMC, we knocked down TASK-1 expression using TASK-1 siRNA. In the siRNA transfected cells, no inhibition of the remaining current by ET-1 was detected compared to control primary

hPASMC (Figure 12A) or to scrambled-siRNA transfected hPASMCs (not shown). The histograms in Figure 12B summarize the effect of ET-1 on I_{KN} calculated at 0 mV, showing that there was no significant inhibition by ET-1 on the remaining current after siRNA-treatment. In addition, the siRNA transfected cells showed a significantly less negative membrane potential (-31 ± 1 mV, $p < 0.001$, $n = 6$) compared to control cells (-51 ± 1 mV, $n = 45$). It is noteworthy that in the siRNA-transfected cells ET-1 did not further change the membrane potential (from -31 ±1 mV to -29 ± 1 mV, $p > 0.05$, $n = 6$) suggesting the crucial role of TASK-1 in the ET-1 pathway. In order to investigate the possible physiological relevance of TASK-1 for ET-1 induced pulmonary vasoconstriction, we analyzed the ET-1-induced pressor response in isolated perfused mouse lungs. ET-1 induced a dose-dependent increase in PA pressure (Figure 13). The PA vasoconstriction was more pronounced when anandamide was given prior to the ET-1. The application of 8 nM ET-1 increased pulmonary arterial pressure (PAP) with 15.6 ± 2.3 mmHg. When anandamide was given prior to ET-1, the increase was 23.8 ± 1.0 mmHg ($p < 0.01$, $n = 5$). These results suggest that ET-1 induced pulmonary vasoconstriction partially via TASK-1 channel inhibition.

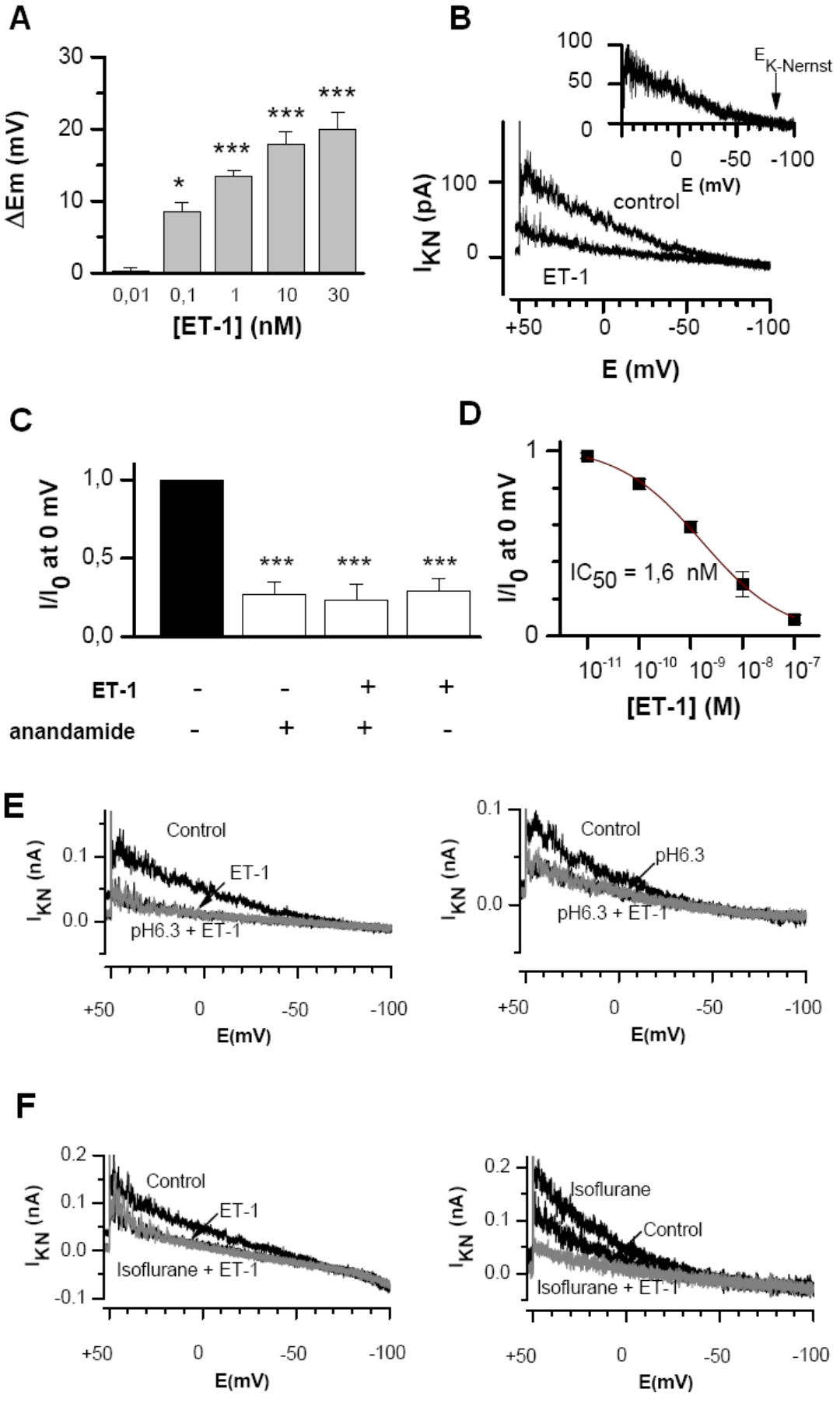
A
ΔEm (mV)
30
20
10
0
*
***
***
***
0,01
0,1
1
10
30
[ET-1] (nM)
B
100
50
0
E K-Nernst
0
-50
-100
E (mV)
I KN (pA)
100
0
control
ET-1
+50
0
-50
-100
E (mV)
C
I/I0 at 0 mV
1,0
0,5
0,0
***
***
***
ET-1
-
-
+
+
anandamide
-
+
+
-
D
I/I0 at 0 mV
1
0
IC50 = 1,6 nM
10-11
10-10
10-9
10-8
10-7
[ET-1] (M)
E
I KN (nA)
0.1
0.0
Control
ET-1
pH6.3 + ET-1
+50
0
-50
-100
E(mV)
I KN (nA)
0.1
0.0
Control
pH6.3
pH6.3 + ET-1
+50
0
-50
-100
E(mV)
F
I KN (nA)
0.2
0.1
0.0
-0.1
Control
ET-1
Isoflurane + ET-1
+50
0
-50
-100
E(mV)
I KN (nA)
0.2
0.1
0.0
Isoflurane
Control
Isoflurane + ET-1
+50
0
-50
-100
E(mV)

Fig. 11. ET-1 blocks I_{KN}. (from Tang et al.; 2009)

(**A**) ET-1 significantly depolarized primary human PASMCs (n = 5 each group; *, $p < 0.05$, ***, $p < 0.001$). (**B**) Effect of 10 nM ET-1 on I_{KN} recorded during ramp, voltage protocol and "difference" currents trace, obtained by subtracting the current amplitudes in the presence of ET-1 from those obtained under control conditions (top). Difference current reversed close to -84 mV, as expected for the K^+-selective conductance under these conditions. (**C**) Effect of anandamide on the ET-1-induced TASK-1 current inhibition. Mean amplitudes of currents ± SEM measured in experiments as indicated. The amplitudes were normalized to the current amplitude obtained with the first recording without drugs (control, black column) (n = 5 each group; ***, $p < 0.001$ difference from control). (**D**) Concentration-response curve for ET-1. I/I_0 is the current in the presence of ET-1 expressed as a fraction of the current prior to ET-1 application. The line is fitted with Hill equation using an IC_{50} of 1.6 ± 0.3 nM. (**E**, left) Representative recordings for I_{KN} after applying ET-1 (10 nM) and after ET-1 application at pH 6.3. (**E**, right) I_{KN} recorded in control, following acidification to pH 6.3 and after application of ET-1 (10 nM) under acidification. (**F**) ET-1 reverses I_{KN} opening by isoflurane (1 mM).

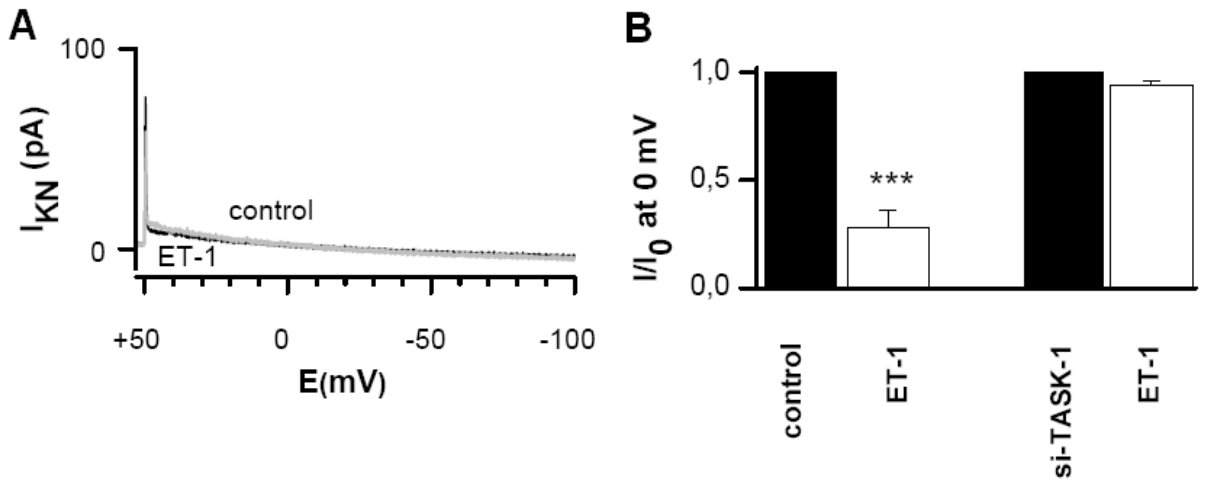

Fig 12. Impact of ET-1 on I_{KN} in TASK-1-siRNA-transfected hPASMCs. (from Tang et al.; 2009)

(**A**) Lack of the ET-1 (10 nM) effect on I_{KN} in TASK-1-siRNA transfected hPASMCs. (**B**) The histogram summarizes the effect of ET-1 on I_{KN} calculated at 0 mV in control and siRNA-transfected primary hPASMCs (n = 6 each group; ***, p < 0.001).

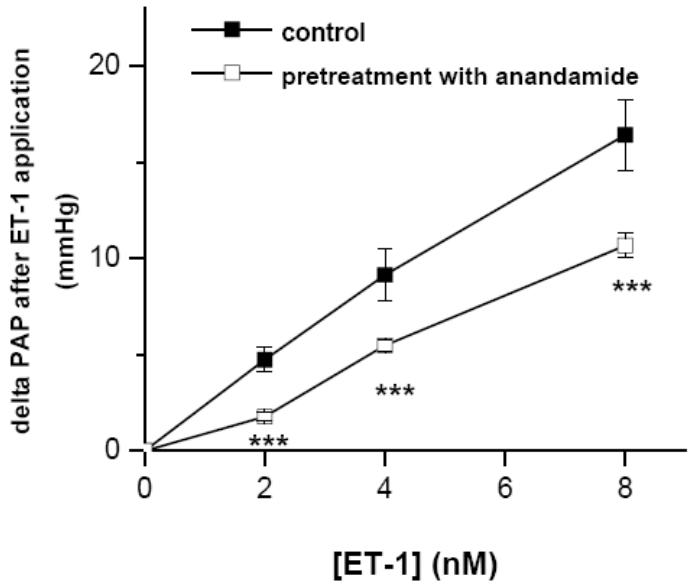

Fig 13. Effect of ET-1 on the isolated perfused mouse lungs (from Tang et al.; 2009; performed by Norbert Weissmann).

ET-1 increased the pulmonary arterial pressure (PAP) in isolated perfused lungs in a dose dependent manner. The ET-1-induced vasoconstriction (delta PAP after ET-1 application) was reduced when anandamide was applied before ET-1 compared to the sole ET-1 treatment (n = 5 each group; ***, p < 0.001).

7.2.2 The ET-1 signaling pathway

In human, ET-1 binds to two types of receptors, ET_A and ET_B. Both G protein-coupled-receptors were detected in PASMCs. In order to investigate which receptor is involved in the inhibition of TASK-1 by ET-1, we used different ET-1 receptor antagonists: BQ123 (ET_A blocker; 1 µM), BQ788 (ET_B blocker; 1 µM), and PD142893 (a non-specific ET_{A+B} blocker; 100 nM). The ET-1 induced TASK-1 inhibition was completely abolished by pre-application of BQ123 and PD142893 (Figure 14A and C). In contrast, pre-application of BQ788 had only a negligible effect on the ET-1-induced inhibition of TASK-1 (Figure 14B and C), suggesting that the ET_A receptor mediates the TASK-1 response to ET-1. Caveolins are involved in multiple cellular processes such as calcium homeostasis(Hardin *et al.*, 2006) and signal transduction(Williams *et al.*, 2004),(Cohen *et al.*, 2004). Moreover, ET_A receptors are localized within caveolae(Chun *et al.*, 1994). Thereby, we investigated the possible involvement of caveolae and phosphorylation of TASK-1 in the ET-1-mediated signal transduction in human PASMCs. PASMC were first analyzed for TASK-1 and caveolins via western blot analysis. In hPASMC we detected caveolin 1, 2 and 3, but the coimmunoprecipitation studies did not indicate any interaction among TASK-1 and these caveolins after ET-1stimulation (Figure 15).

In order to further assess the mechanisms involved in ET-1-induced TASK-1 inhibition, hPASMCs were incubated for 10 min with ET-1 (10 nM). No differences in the tyrosine phosphorylation of TASK-1 was observed when ET-treated and untreated groups were compared (n = 3; Figure 16). In contrast, the incubation with ET-1 stimulated the threonine phosphorylation of TASK-1, as was evident in TASK-1 immunoprecipitates probed with an anti-phosphothreonine antibody (Figure 16). Protein loading equivalence was demonstrated by probing immunoprecipitates with an anti–TASK-1 antibody (Figure 16). In patch-clamp studies, various PKC inhibitors, including Ro318220 (1 µM), Gö6983 (10 nM) and rottlerin (10 nM) were used on the non-inactivating current

response to ET-1 to confirm the PKC action. The pretreatment of the cells with the broad-spectrum PKC blocker Ro318220 and the classic, fast acting PKC inhibitor Gö6983 abolished the effect of ET-1 on the TASK-1 current (Figure 17). Rottlerin, a selective PKCδ inhibitor, partially blocked the inhibition of TASK-1 by ET-1. Consistent with the effects of the PKC inhibitors, preincubation with the PKA inhibitor KT5720, did not lead to any change in ET-1 dependent TASK-1 inhibition (not shown). Collectively, these results lead to the suggestion that in hPASMC TASK-1 channels are inhibited by ET-1 primarily through the PKC-dependent pathways.

PKC may be activated in response to diacylglycerol (DAG) and inositol 1,4,5-triphosphate (IP_3)-stimulated increased cytosolic calcium generated via phospholipase C (PLC). To address the ET-1 signaling pathway downstream of the G protein-coupled receptor ET_A, we combined pharmacological approaches with patch-clamp studies. First, we investigated the involvement of PLC-dependent signaling pathway(s) using the PLC antagonist U-73122 on the ET-1 induced TASK-1 inhibition. Pre-application of U-73122 in hPASMCs completely abolished the effect of ET-1 (10 nM) on I_{KN} (Figure 18A). Phosphatidylinositol 4,5- biphosphate (PIP_2) serves as a substrate for the hydrolysis by PLC to produce inositol 1,4,5-triphosphate (IP_3) and diacylglycerol (DAG). Thus, hPASMCs were dialyzed with the PIP_2 scavenger poly-lysine (30 µg/ml), widely used to demonstrate the regulation of channels by endogenous PIP_2 and then superfused with ET-1 (10 nmol/L). Cells dialyzed with the internal control solution were used as a control. The application of poly-lysine alone significantly reduced the current density to or below the level recorded after an ET-1 application. When ET-1 was simultaneously applied, it did not block TASK-1 (Figure 18B). Next, in order to determine whether IP_3 or DAG is required for the PKC activation, we incubated hPASMC with the DAG kinase inhibitor R-59949 (30 µM) prior to ET-1 (10 nM). R-59949 inhibited TASK-1 (Figure 18C and D). Similar data were obtained when OAG (a DAG analogue, 100 µM) was applied prior to ET-1 in hPASMC. Application of OAG alone led to a significant inhibition of the TASK-1 current, similar to the effect of ET-1 alone. Thus, the TASK-1 current was not further blocked when ET-1 was additionally applied, as shown in Figure

18E and F. Taken together; these results indicate that the ET_A-PLC-PIP_2-DAG-PKC pathway is essential for the inhibition of TASK-1 by ET-1 in primary human PASMCs.

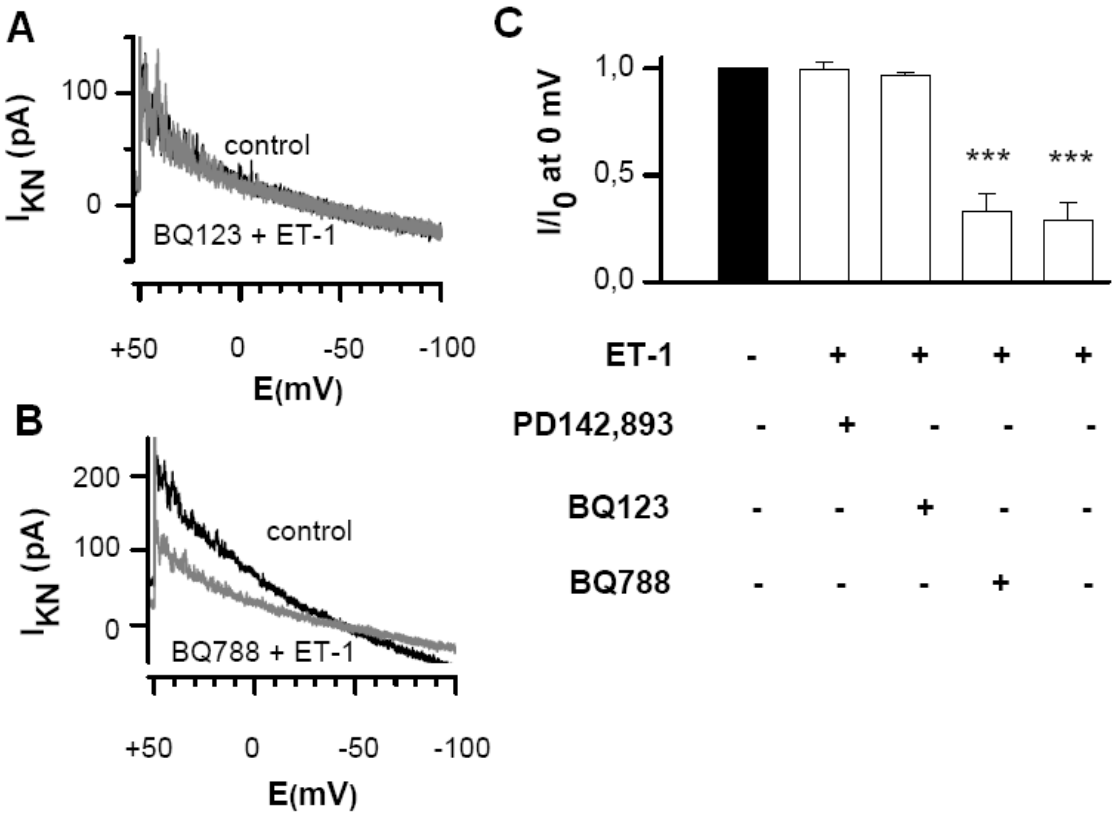

Fig 14. Blockade of the ET_A receptor abolishes the ET-1 effect. (from Tang et al.; 2009)

(**A**) and (**B**) Non-inactivating current TASK-1 channels in response to an ET-1 application in the presence of BQ123 (ET_A receptor antagonist; 1 μM) or BQ788 (ET_B receptor antagonist; 1 μM). Human PASMCs were pretreated for 1 h with the inhibitors prior to the addition of ET-1 (10 nM). (**C**) The histogram summarizes the effect of ET-1 on the TASK-1 current after pretreatment of hPASMCs with PD142893 (ET_{A+B} antagonist 100nM), BQ123 or BQ788 (1 μM) (n = 6 each group; ***, $p < 0.001$ difference from ET-1-untreated cells). I/I_0 is the current in the presence of ET-1 expressed as a fraction of the current prior to ET-1 application.

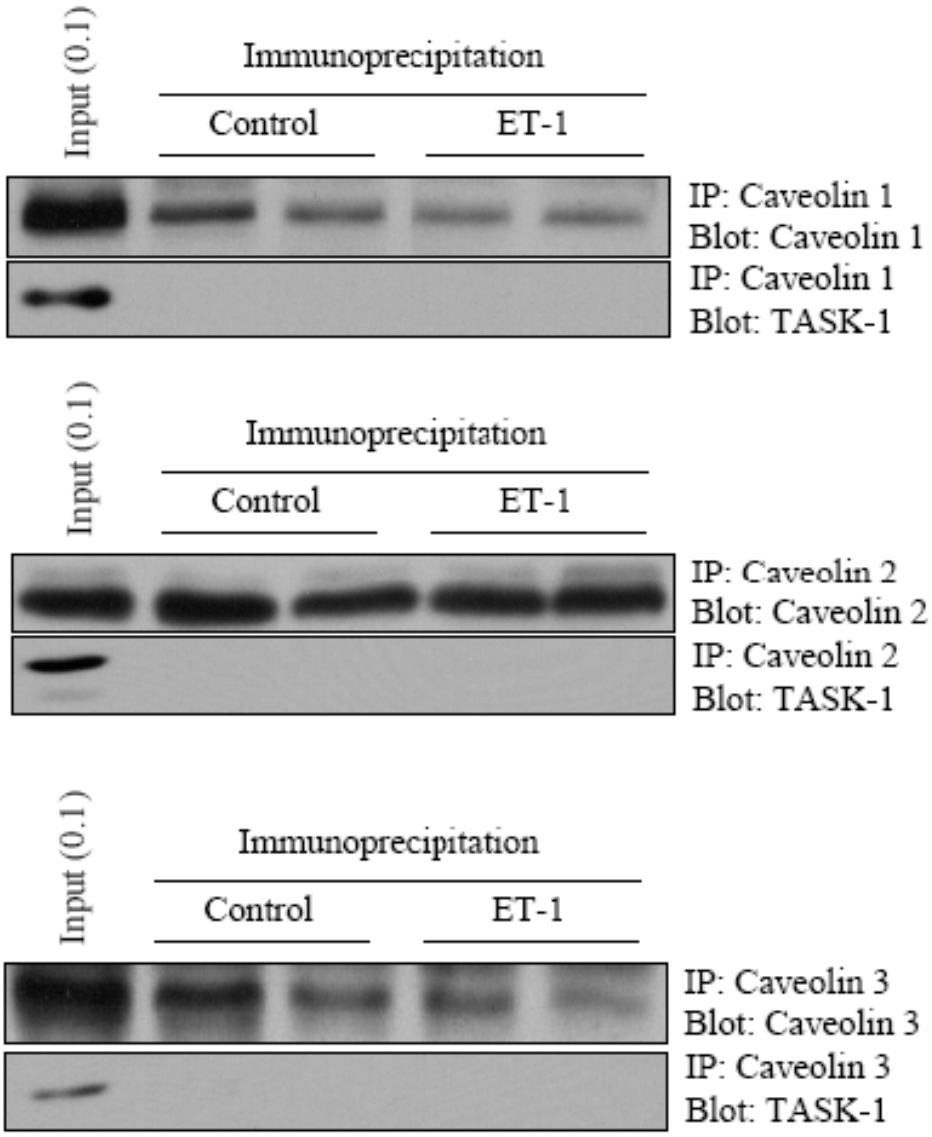

Fig 15. Effects of ET-1 on TASK-1 with caveolin (from Tang et al.; 2009; performed by Rory E. Morty).

Primary human PASMCs were treated for 10 min with or without ET-1 (10 nM). Homogenates were immunoprecipitated with anti-TASK-1 antibody submitted to SDS-PAGE. Membranes were probed for caveolin-1, 2 or 3, and TASK-1.

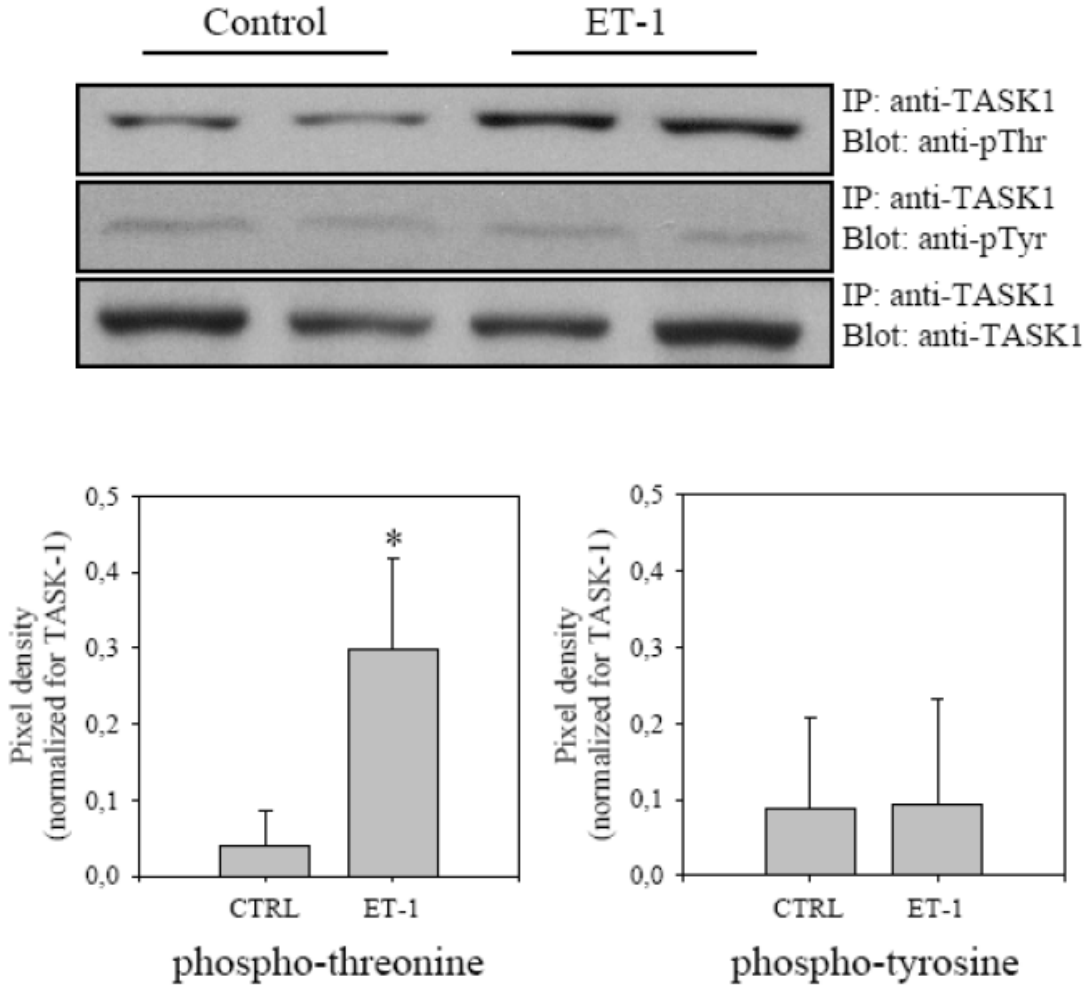

Fig 16. PKC-dependent phosphorylation of TASK-1 by ET-1. (from Tang et al.; 2009) Representative results of the threonine (left) and tyrosine (right) phosphorylation of TASK-1 in ET-1-treated and untreated (control) hPASMCs. Protein loading equivalence is shown by probing immunoprecipitates with an anti-TASK-1 antibody in the lower panel.

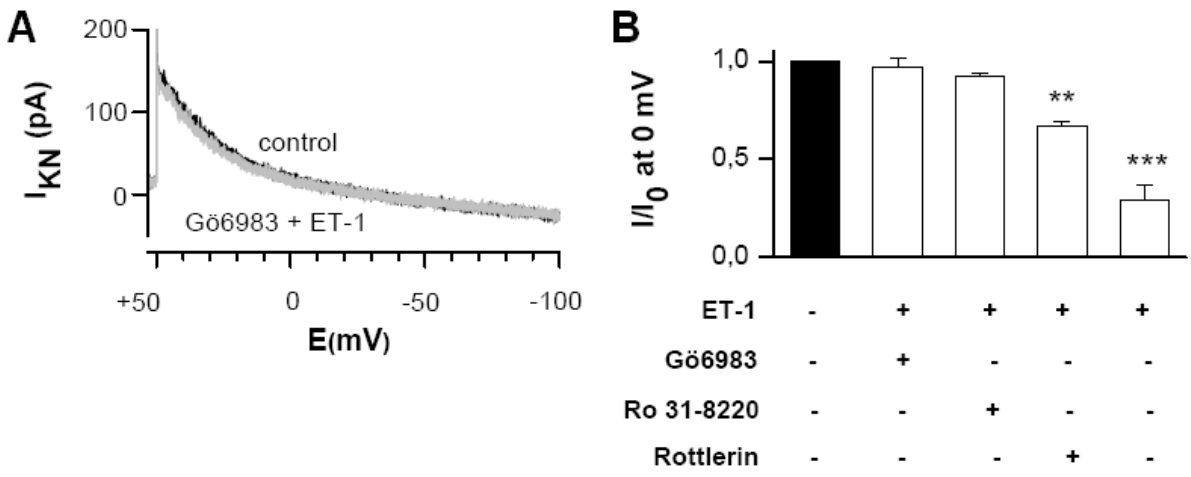

Fig 17. Impacts of PKC inhibitors on the ET-1 effect. (from Tang et al.; 2009)

(**A**) Representative traces show the lack of ET- 1 (10nM) effect on TASK-1 after 1 h preincubation with Gö6983 (10 nM). (**B**) The histogram summarizing the effect of ET-1 on the TASK-1 current after pretreatment of hPASMCs with Ro318220 (1μM), Gö6983 or rottlerin (10 nM) (n = 6 each group; **, $p < 0.01$; ***, $p < 0.001$ difference from ET-1-untreated cells). I/I_0 is the current in the presence of ET-1 expressed as a fraction of the current prior to ET-1 application.

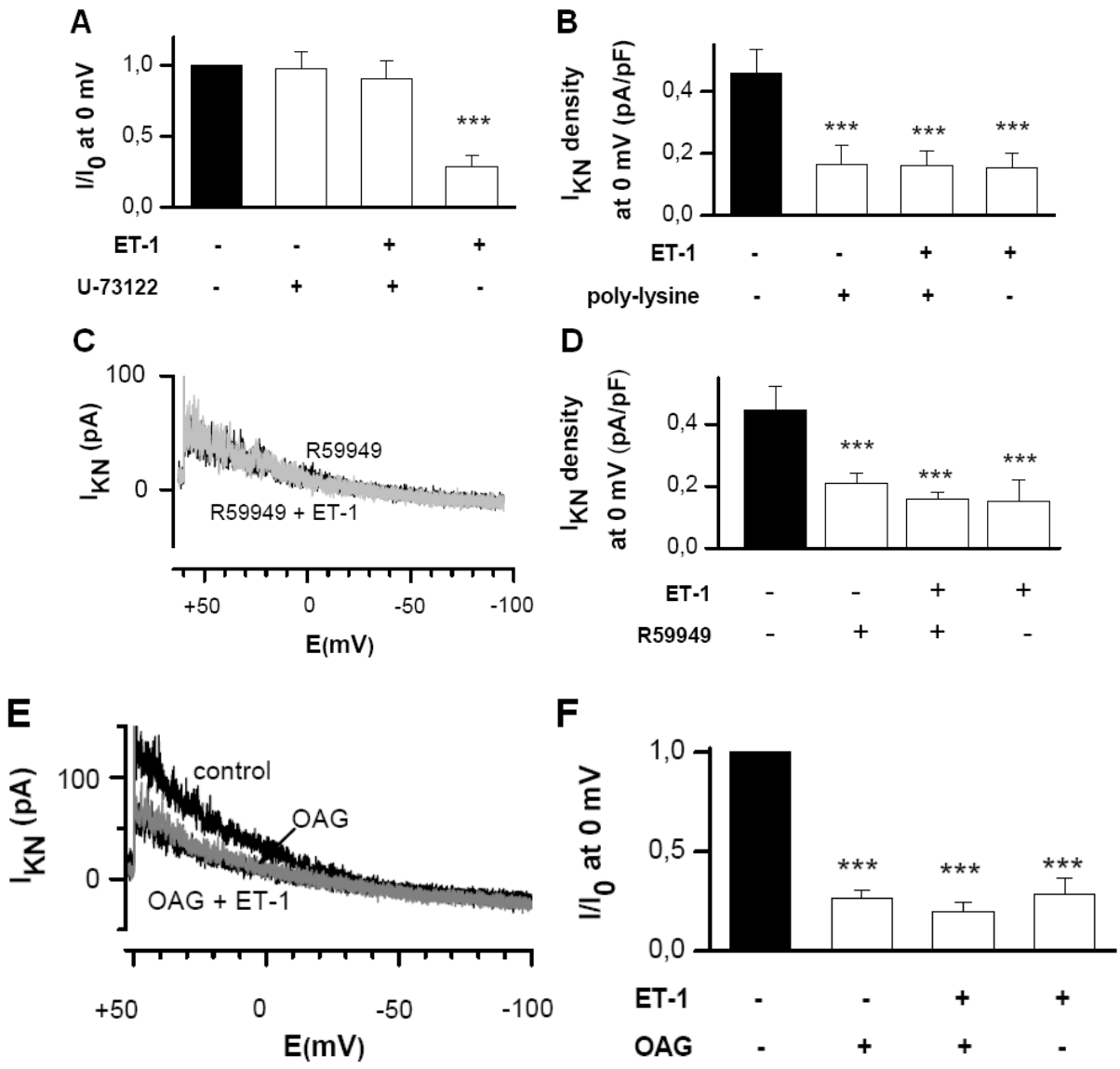

Fig 18. Downstream signaling pathway of the ET_A receptors. (from Tang et al.; 2009)

(**A**) and (**B**) Mean amplitudes of currents ± SEM measured in experiments as indicated. The amplitudes were normalized to the current amplitude obtained with the first recording without drugs (control, black column). (**C**) Non-inactivating current of TASK-1 channels in response to the application of the DAG kinase inhibitor R-59949 and R-59949 + ET-1. (**D**) Mean amplitudes of the current density ± SEM. Black column shows the control without preincubation with R-59949. (**E**) Non-inactivating current of TASK-1 channels in response to the application of the DAG analog OAG and OAG + ET-1. (**F**) Mean currents amplitudes ± SEM measured in experiments as indicated. The

amplitudes were normalized to the current amplitude obtained from the recording without drugs (control, black column) (n = 5 each group; ***, $p < 0.001$ difference from control).

8. Discussion

8.1. Two-Pore domain potassium channels in hPASMC

Smooth muscle cells have negative resting potentials that are important for the regulation of the excitability and the contractile tissue properties. K^+ channels play an essential role in the regulation of the resting membrane potential and are able to drive the resting membrane potential near the K^+ equilibrium potential. Different types of K^+ channels have been identified in pulmonary artery smooth muscle cells (PASMCs), including voltage-gated K^+ channels (K_V) (Post *et al.*, 1995),(Weir *et al.*, 1995), (Platoshyn *et al.*, 2004), large-conductance Ca^{2+}–activated channels (Albarwani *et al.*, 1994),(Peng *et al.*, 1999), and ATP-dependent channels (K_{ATP}) (Nelson *et al.*, 1995). The three kinds of channels are predominantly activated when the cell is stimulated. In contrast, a new group of recently described K^+ channels, the background (leak) two-pore-domain (2P) K^+ channels, are give rise to K^+-selective currents that are open at all voltages when these superfamily of 2-PK channels are functionally expressed (Gurney *et al.*, 2003),(Gardener *et al.*, 2004). It has become clear that the newly identified KCNK family of K^+ channel subunits also contribute to the K^+ current in smooth muscle cells (Gurney *et al.*, 2003),(Gardener *et al.*, 2004). A decrease in the leak K^+ conductance leads to a cell depolarization that enhances the open probability of L-type Ca^{2+} channels in smooth muscle cells, resulting in a periodic Ca^{2+} entry and finally in vasoconstriction.

In this study, we demonstrated the expression of TASK-1 mRNAs and proteins in hPASMCs. Moreover, our antibody staining shows a TASK-1 expression at the membrane surface, compatible with a functional role in mediating the membrane K^+ currents. We have found an anandamide-sensitive conductance in primary hPASMC that had properties similar to the TASK-1 channels. The native conductance shows an outward rectification in the low external K^+ solution, instantaneous and noninactivating. It is activated by alkalotic pH or potentiated by isoflurane, and blocked by anandamide

and Zn^{2+}. It is insensitive to TEA and 4-AP. Transfection of TASK-1 siRNA into hPASMC significantly depolarizes the resting membrane potential and abolishes the effect of pH and anandamide. Furthermore, we are able to show the hypoxia sensitivity of the TASK-1 current. We conclude that TASK-1 channels are responsible for the hypoxia- and pH-sensitive, voltage-independent background conductance that sets the resting membrane potential in hPASMC.

The results of our experiments exclude the possibility that classical voltage-sensitive, Ca^{2+}-sensitive, and ATP-sensitive K^+ channels play a significant role in mediating the observed pH-induced changes in the membrane potential. TASK-1 is very sensitive to variations in the extracellular pH in a narrow physiological range which has been reported in many different cell types (Duprat *et al.*, 1997),(Buckler *et al.*, 2000),(Reyes *et al.*, 1998). Local pH changes caused by physiological or pathophysiological conditions, such as hypo- or hyperventilation or ischemia in the pulmonary vascular bed, may result in acidosis or alkalosis and lead to changes in the pulmonary artery pressure. Our data suggest that the effects on the pH-sensitive ion channels may also explain the acidosis-induced vasoconstriction and the alkalosis-induced vasodilatory responses. Furthermore, anandamide, a selective TASK-1 blocker, significantly reduces I_{KN} and causes a depolarization similar to that seen at pH 6.4. This observation is consistent with results reported in earlier studies (Gurney *et al.*, 2003),(Maingret *et al.*, 2001),(Leonoudakis *et al.*, 1998). In a symmetrical K^+ concentration, the I/V curve for I_{KN} becomes linear and anandamide inhibits a voltage-independent current with a reversal potential close to 0 mV, demonstrating that TASK-1 behaves as a pure K^+-selective leak channel. Taken together, these data provide an unequivocal biophysical and pharmacological evidence for the functional expression of TASK-1 in primary hPASMC.

The application of TASK-1 small interfering RNA provides further evidence to link the resting membrane potential and TASK-1 channel. The resting membrane potential is significantly decreased in transfected cells. Moreover, the loss of sensitivity of the membrane potential to a significant depolarization by anandamide and pH 6.4, or to a significant hyperpolarization by pH 8.4 in transfected cells, strongly implicates TASK-1 as a major contributor to the resting membrane potential.

Acute hypoxic inhibition of K^+ channels is a critical step in the regulatory processes designed to link the lowering of O_2 levels to cellular responses. It is often questioned whether the K^+ channels are active at sufficiently negative potentials to set the resting membrane potential of PASMC and whether K^+ channels are able to mediate hypoxic pulmonary vasoconstriction. Since hypoxia depolarizes pulmonary artery smooth muscle cells (Post *et al.*, 1992), it is thought that an oxygen-sensitive component of the resting membrane potential may contribute to this hypoxia-induced pulmonary vasoconstriction (HPV). Importantly, I_{KN} in both rabbit (Osipenko *et al.*, 1997) and human PASMC is inhibited reversibly by acute hypoxia, which is compatible with it being responsible for the oxygen sensitivity of the membrane potential. Based on the compelling evidence, we know that TASK-1 is a major contributor to I_{KN} and that its inhibition by hypoxia underlies hypoxia-induced depolarization. These discoveries are consistent with the role of the TASK channels in the background conductances of other cell types, such as I_{KSO} (a ‘‘standing-outward’’ K^+ current, an outwardly rectifying potassium current) in cerebellar granule neurons (Millar *et al.*, 2000) and the oxygen-sensitive current in cells of the carotid body (Buckler *et al.*, 2000).

8.2. TASK-1 regulation by endothelin-1

Endothelin plays a central role in the pathogenesis of pulmonary hypertension and has been extensively studied. Our results provide evidence that endothelin modulates the native background two-pore domain K^+ channel TASK-1 in primary human pulmonary artery smooth muscle cells which sets their membrane potential, as above shown by means of TASK-1-siRNA studies. Consequently, ET-1 depolarizes the resting membrane potential of hPASMCs at clinically relevant concentrations by a dose-dependent inhibition of TASK-1. These effects are abolished by antagonists of the G protein-coupled-receptor ET_A, the PIP_2 scavenger and the inhibitors of PLC, DAG kinase, and PKC.

The effects of endothelin on pulmonary vessels is the matter of a continued interest, because an activated endothelin system significantly contributes to the pathological changes in pulmonary hypertension (Stewart *et al.*, 1991),(Giaid *et al.*, 1993). Endothelin receptor antagonists have been shown to be effective for the therapy of pulmonary arterial hypertension (Rubin *et al.*, 2002). Circulating or lung tissue levels of ET-1 are elevated in animal models of PAH (Miyauchi *et al.*, 1993),(Ivy *et al.*, 1998),(Frasch *et al.*, 1999),(Nakanishi *et al.*, 1999) as well as in human PAH (Stewart *et al.*, 1991),(Giaid *et al.*, 1993),(Kumar *et al.*, 1996),(Yoshibayashi *et al.*, 1991). In addition, a correlation between an increased ET-1 expression in the lung of patients with pulmonary hypertension and the severity of the disease was demonstrated (Giaid *et al.*, 1993). Although multiple evidences indicate that the endothelin system plays a key role in the pathogenesis of pulmonary hypertension, the molecular targets of ET-1 have not been clearly defined in detail until now. Under normoxic conditions, the acute ET-1-induced vasoconstriction occurs via a Ca^{2+}-dependent mechanism, mainly by Ca^{2+} influx through voltage-activated calcium channels, secondary to K^+ channel inhibition and membrane depolarization. To date, the involvement of voltage-activated K channels (Shimoda *et al.*, 2001) or ATP-dependent K channels (Park *et al.*, 2005) has been established. In human PASMC, our previous study demonstrated that only TASK-1

channels, a member of the background two-pore domain K^+ channel family are identified. If these channels are functionally expressed, they give rise to the K^+-selective current that is open at all voltages, in contrast to the K_V or K_{ATP} channels whose activity is controlled by voltage or metabolic regulation. In fact, background K^+ channels such as TASK-1 set the resting membrane potential in excitable cells (Millar *et al.*, 2000),(Backx *et al.*, 1993),(Patel *et al.*, 1999),(Talley *et al.*, 2002),(Talley *et al.*, 2003),(Sirois *et al.*, 2000). Due to the fact that TASK-1 is active at rest in hPASMC, its inhibition would lead to a cell depolarization that enhances the open probability of the L-type Ca^{2+} channels in smooth muscle cells, causing a periodical Ca^{2+} entry as well as vasoconstriction. We have now identified the TASK-1 channel as an important target for ET-1 at clinically relevant concentrations. We have established a role for the TASK-1 channels in the ET-1-induced membrane depolarization in primary human PASMCs, using TASK-1-siRNA. This might represent an important pathway explaining a part of the vasoconstrictive and proliferative properties of ET-1. In addition, these findings might be further supported using the isolated perfused mouse lung model, in which the effect of anandamide on ET-1-induced pulmonary vasoconstriction was investigated. When anandamide was given prior to ET-1, the vasoconstrictive response was augmented. This suggests that anandamide and ET-1 have an additive effect on the TASK-1 inhibition. However, it has to be taken into account that the endocannabinoid anandamide, besides TASK-1, also acts on specific cannabinoid (CB1) and on vanilloid receptors (VR1). Furthermore, in the mouse model, the expression of other possible anandamide-sensitive two-pore domain channels has not been fully characterized until now.

ET-1 has been shown to affect several different types of ion channels in vascular smooth muscle cells. Various signaling pathways have been implicated in these effects. In our study, we have specifically examined the signaling pathway involved in the ET-1-induced TASK-1 inhibition in primary human PASMCs. We have found that antagonists of the G protein-coupled-receptor ET_A fully abolish the TASK-1 inhibition in response to ET-1. The molecular basis of the K^+ channel inhibition by an agonist that acts on the Gq-coupled receptor upstream of PKC is reasonably well defined for some

K^+ channels (Suh *et al.*, 2004),(Lei *et al.*, 2003) but has been controversially defined for background two-pore domain K^+ channels (Mathie, 2007) and in particular not investigated in native vascular cells yet. Antagonists of PKC but not PKA inhibit the ET-1 effect on TASK-1, suggesting that PKC mediates the agonist-induced inhibition. These results show that the binding of ET-1 to G protein–coupled ET_A receptors activates PKC, thereby, modulating the ion channels. Our data indicate that ET-1 can stimulate the serine or threonine phosphorylation of TASK-1, and are consistent with the detection of phosphoserine in TASK-1(O'Kelly *et al.*, 2002), and the presence of consensus serine and threonine protein kinase A and C phosphorylation sites in the TASK-1 peptide (Duprat *et al.*, 1997). While a tyrosine kinase consensus site is also present in the TASK-1 peptide, ET-1 does not effect the tyrosine phosphorylation of TASK-1.

Several studies have examined the mechanism by which a G-protein coupled receptor agonist may inhibit two-pore domain K^+ channels via PKC. These studies suggest that an agonist-induced inhibition of the two-pore domain K^+ channels is due to ATP-dependent pathways (Enyeart *et al.*, 2005), by depletion of the phosphatidylinositol 4,5-bisphosphate (PIP_2) levels (Lopes *et al.*, 2005), directly by a direct action of diacylglycerol (DAG) and phosphatidic acid that are generated via PLC (Chemin *et al.*, 2003) or by elevated intracellular Ca^{2+} levels (Enyeart *et al.*, 2005). Moreover, a very recent study proposes a direct interaction of Gαq with TASK-1 in a mammalian heterologous expression system (Chen *et al.*, 2006). The results obtained from different laboratories suggest the possibility that the two-pore domain channels may be modulated not by a single mechanism but via distinct pathways in different cell types. We have found that the inhibition of the phospholipase C abolishes the ET-1 effect on TASK-1 indicating that PLC is required, as also shown in Xenopus laevis oocytes (Czirjak *et al.*, 2001) and in contrast to the report about a mammalian heterologous expression system (Talley *et al.*, 2002). Additional evidence comes from the use of COS-7 cells expressing TREK-2 and muscarinic receptor M_3, in which the same PLC inhibitor was applied to prevent acetylcholine induced inhibition of TREK-2 (Kang *et al.*, 2006). The inhibitory effect of the PIP_2 scavenger on TASK-1, observed in this study, confirms previously reported results obtained from different two-pore domain K^+

channels expressed in *Xenopus* oocytes (Lopes *et al.*, 2005) and strongly suggests that PIP_2 hydrolysis by PLC indeed affects the channel activity. Moreover, we have showed that the downstream product of the PIP_2 hydrolysis, DAG, underlies the agonist-induced inhibition of TASK-1 in hPASMCs. These results are further supported by our experiments showing that the DAG-kinase inhibitors abolish the ET-1 effect on TASK-1.

9. Conclusion and outlook

We demonstrate that TASK-1, a member of the 2-PK channel superfamily is expressed in human primary PASMC. TASK-1 controls the resting membrane potential, thus, implicating the TASK-1 channels in the regulation of the pulmonary vascular tone.TASK-1 might be also the perfect candidate for the initiation of hypoxia–induced depolarization in PASMC. Moreover, the TASK-1 modulation by the Gαq pathway is achieved by signaling rather than direct interaction between PIP_2 and TASK-1 in primary human PASMCs (Lopes *et al.*, 2005)(Figure 19). Additionaly, we report here the involvement of the background two-pore domain K^+ channel TASK-1 in the endothelin-1-mediated depolarization in native human PASMC. It is tempting to hypothesize that the inhibition of the voltage-independent TASK-1 channel by endothelin in human PASMCs contributes to the development of human pulmonary hypertension.

During the last decade, important breakthroughs about the role of the K_{2P} channel family in the cardiopulmonary vascular system emerged. Now there exist a clear evidence for two pore-domain potassium channels in the heart and lung. They are likely to contribute to cardiopulmonary function through their regulation by stretch, hypoxia, pH, prostacyclin analogs (such as iloprost and treprostinil), and neurotransmitters.

Although numerous other members of the K_{2P} family have been shown to be expressed in various parts of the cardiopulmonary vascular system, their physiological importance is still obscure, partly due to the lack of pharmacological tools that possess selectivity for these channels. Genetic approaches using knockout animals and RNA interference technology have provided helpful data and will be invaluable in the future for unraveling the physiological functions of the many K_{2P} channels that appear to be expressed in the muscle and endothelial cells of the cardiopulmonary vascular system. Our understanding of the K_{2P} channels in the cardiopulmonary vascular system is still embryonic, but it is clear that these channels are likely to be important in the normal physiological regulation of the heart-lung and the arteries as well as in pathological

processes. Although the pharmacology of the K_{2P} channels is currently poor, as our understanding of the channels improves, new drugs with greater selectivity are likely to emerge. The K_{2P} channels in the cardiopulmonary vascular system therefore offer a high potential for the future development of therapeutic agents against cardiovascular diseases and pulmonary arterial hypertension.

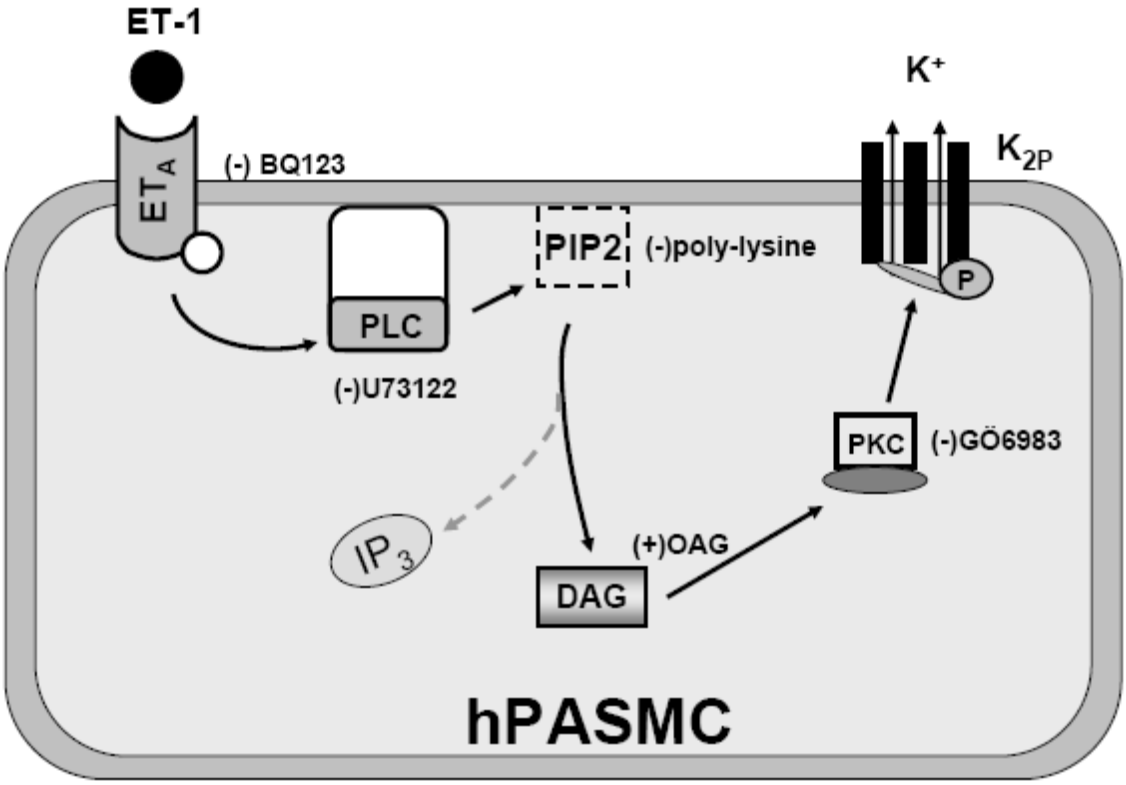

Fig. 19. Schematic presentation of the ET-1 signaling pathway in hPASMCs. (from Tang et al.; 2009)

ET-1 binds to the G protein-coupled-receptor (Gαq) ET_A, leading to the protein kinase C (PKC)-induced phosphorylation of TASK-1 channels through phospholipase C (PLC), phosphatidylinositol 4,5-biphosphate (PIP_2) and diacylglycerol (DAG). (+) indicate agonist and (-) indicate antagonist effects.

Appendix

10.1. References

ALBARWANI, S., ROBERTSON, B.E., NYE, P.C. & KOZLOWSKI, R.Z. (1994). Biophysical properties of Ca^{2+}- and Mg-ATP-activated K^+ channels in pulmonary arterial smooth muscle cells isolated from the rat. *Pflugers Arch*, **428,** 446-54.

ARCHER, S.L., HUANG, J.M., REEVE, H.L., HAMPL, V., TOLAROVA, S., MICHELAKIS, E. & WEIR, E.K. (1996). Differential distribution of electrophysiologically distinct myocytes in conduit and resistance arteries determines their response to nitric oxide and hypoxia. *Circ Res*, **78,** 431-42.

ARCHER, S.L., SOUIL, E., DINH-XUAN, A.T., SCHREMMER, B., MERCIER, J.C., EL YAAGOUBI, A., NGUYEN-HUU, L., REEVE, H.L. & HAMPL, V. (1998). Molecular identification of the role of voltage-gated K^+ channels, Kv1.5 and Kv2.1, in hypoxic pulmonary vasoconstriction and control of resting membrane potential in rat pulmonary artery myocytes. *J Clin Invest*, **101,** 2319-30.

BACKX, P.H. & MARBAN, E. (1993). Background potassium current active during the plateau of the action potential in guinea pig ventricular myocytes. *Circ Res*, **72,** 890-900.

BAI, X., BUGG, G.J., GREENWOOD, S.L., GLAZIER, J.D., SIBLEY, C.P., BAKER, P.N., TAGGART, M.J. & FYFE, G.K. (2005). Expression of TASK and TREK, two-pore domain K^+ channels, in human myometrium. *Reproduction*, **129,** 525-30.

BAYLISS, D.A., TALLEY, E.M., SIROIS, J.E. & LEI, Q. (2001). TASK-1 is a highly modulated pH-sensitive 'leak' K^+ channel expressed in brainstem respiratory neurons. *Respir Physiol*, **129,** 159-74.

BECKETT, E.A., HAN, I., BAKER, S.A., HAN, J., BRITTON, F.C. & KOH, S.D. (2008). Functional and molecular identification of pH-sensitive K^+ channels in murine urinary bladder smooth muscle. *BJU Int*, **102,** 113-24.

BUCKINGHAM, S.D., KIDD, J.F., LAW, R.J., FRANKS, C.J. & SATTELLE, D.B. (2005). Structure and function of two-pore-domain K^+ channels: contributions from genetic model organisms. *Trends Pharmacol Sci*, **26,** 361-7.

BUCKLER, K.J. & HONORE, E. (2005). The lipid-activated two-pore domain K^+ channel TREK-1 is resistant to hypoxia: implication for ischaemic neuroprotection. *J Physiol*, **562,** 213-22.

BUCKLER, K.J., WILLIAMS, B.A. & HONORE, E. (2000). An oxygen-, acid- and anaesthetic-sensitive TASK-like background potassium channel in rat arterial chemoreceptor cells. *J Physiol*, **525 Pt 1,** 135-42.

CHEMIN, J., GIRARD, C., DUPRAT, F., LESAGE, F., ROMEY, G. & LAZDUNSKI, M. (2003). Mechanisms underlying excitatory effects of group I metabotropic glutamate receptors via inhibition of 2P domain K^+ channels. *Embo J*, **22,** 5403-11.

CHEMIN, J., PATEL, A.J., DUPRAT, F., LAURITZEN, I., LAZDUNSKI, M. & HONORE, E. (2005). A phospholipid sensor controls mechanogating of the K^+ channel TREK-1. *Embo J*, **24,** 44-53.

CHEN, S.J., CHEN, Y.F., MENG, Q.C., DURAND, J., DICARLO, V.S. & OPARIL, S. (1995). Endothelin-receptor antagonist bosentan prevents and reverses hypoxic pulmonary hypertension in rats. *J Appl Physiol*, **79,** 2122-31.

CHEN, X., TALLEY, E.M., PATEL, N., GOMIS, A., MCINTIRE, W.E., DONG, B., VIANA, F.,

GARRISON, J.C. & BAYLISS, D.A. (2006). Inhibition of a background potassium channel by Gq protein alpha-subunits. *Proc Natl Acad Sci U S A*, **103,** 3422-7.

CHUN, M., LIYANAGE, U.K., LISANTI, M.P. & LODISH, H.F. (1994). Signal transduction of a G protein-coupled receptor in caveolae: colocalization of endothelin and its receptor with caveolin. *Proc Natl Acad Sci U S A*, **91,** 11728-32.

CLAPP, L.H., DAVEY, R. & GURNEY, A.M. (1993). ATP-sensitive K^+ channels mediate vasodilation produced by lemakalim in rabbit pulmonary artery. *Am J Physiol*, **264,** H1907-15.

COHEN, A.W., HNASKO, R., SCHUBERT, W. & LISANTI, M.P. (2004). Role of caveolae and caveolins in health and disease. *Physiol Rev*, **84,** 1341-79.

CZIRJAK, G. & ENYEDI, P. (2002). Formation of functional heterodimers between the TASK-1 and TASK-3 two-pore domain potassium channel subunits. *J Biol Chem*, **277,** 5426-32.

CZIRJAK, G., PETHEO, G.L., SPAT, A. & ENYEDI, P. (2001). Inhibition of TASK-1 potassium channel by phospholipase C. *Am J Physiol Cell Physiol*, **281,** C700-8.

DAVIE, N., HALEEN, S.J., UPTON, P.D., POLAK, J.M., YACOUB, M.H., MORRELL, N.W. & WHARTON, J. (2002). ET_A and ET_B receptors modulate the proliferation of human pulmonary artery smooth muscle cells. *Am J Respir Crit Care Med*, **165,** 398-405.

DUPRAT, F., LESAGE, F., FINK, M., REYES, R., HEURTEAUX, C. & LAZDUNSKI, M. (1997). TASK, a human background K^+ channel to sense external pH variations near physiological pH. *Embo J*, **16,** 5464-71.

EDDAHIBI, S., GUIGNABERT, C., BARLIER-MUR, A.M., DEWACHTER, L., FADEL, E.,

DARTEVELLE, P., HUMBERT, M., SIMONNEAU, G., HANOUN, N., SAURINI, F., HAMON, M. & ADNOT, S. (2006). Cross talk between endothelial and smooth muscle cells in pulmonary hypertension: critical role for serotonin-induced smooth muscle hyperplasia. *Circulation*, **113,** 1857-64.

ENYEART, J.J., DANTHI, S.J., LIU, H. & ENYEART, J.A. (2005). Angiotensin II inhibits bTREK-1 K^+ channels in adrenocortical cells by separate Ca^{2+}- and ATP hydrolysis-dependent mechanisms. *J Biol Chem*, **280,** 30814-28.

EVANS, A.M., OSIPENKO, O.N. & GURNEY, A.M. (1996). Properties of a novel K^+ current that is active at resting potential in rabbit pulmonary artery smooth muscle cells. *J Physiol*, **496 (Pt 2),** 407-20.

FRASCH, H.F., MARSHALL, C. & MARSHALL, B.E. (1999). Endothelin-1 is elevated in monocrotaline pulmonary hypertension. *Am J Physiol*, **276,** L304-10.

GALIE, N., MANES, A. & BRANZI, A. (2004). The endothelin system in pulmonary arterial hypertension. *Cardiovasc Res*, **61,** 227-37.

GARDENER, M.J., JOHNSON, I.T., BURNHAM, M.P., EDWARDS, G., HEAGERTY, A.M. & WESTON, A.H. (2004). Functional evidence of a role for two-pore domain potassium channels in rat mesenteric and pulmonary arteries. *Br J Pharmacol*, **142,** 192-202.

GIAID, A., YANAGISAWA, M., LANGLEBEN, D., MICHEL, R.P., LEVY, R., SHENNIB, H., KIMURA, S., MASAKI, T., DUGUID, W.P. & STEWART, D.J. (1993). Expression of endothelin-1 in the lungs of patients with pulmonary hypertension. *N Engl J Med*, **328,** 1732-9.

GOLDSTEIN, S.A., WANG, K.W., ILAN, N. & PAUSCH, M.H. (1998). Sequence and function of the two P domain potassium channels: implications of an emerging superfamily. *J Mol Med*, **76,** 13-20.

GOTO, K., KASUYA, Y., MATSUKI, N., TAKUWA, Y., KURIHARA, H., ISHIKAWA, T., KIMURA, S., YANAGISAWA, M. & MASAKI, T. (1989). Endothelin activates the dihydropyridine-sensitive, voltage-dependent Ca^{2+} channel in vascular smooth muscle. *Proc Natl Acad Sci U S A*, **86,** 3915-8.

GULER, A.D., LEE, H., IIDA, T., SHIMIZU, I., TOMINAGA, M. & CATERINA, M. (2002). Heat-evoked activation of the ion channel, TRPV4. *J Neurosci*, **22,** 6408-14.

GURNEY, A. & MANOURY, B. (2009). Two-pore potassium channels in the cardiovascular system. *Eur Biophys J*, **38,** 305-18.

GURNEY, A.M. & JOSHI, S. (2006). The role of twin pore domain and other K^+ channels in hypoxic pulmonary vasoconstriction. *Novartis Found Symp*, **272,** 218-28; discussion 228-33, 274-9.

GURNEY, A.M., OSIPENKO, O.N., MACMILLAN, D., MCFARLANE, K.M., TATE, R.J. & KEMPSILL, F.E. (2003). Two-pore domain K channel, TASK-1, in pulmonary artery smooth muscle cells. *Circ Res*, **93,** 957-64.

HAMILL, O.P., MARTY, A., NEHER, E., SAKMANN, B. & SIGWORTH, F.J. (1981). Improved patch-clamp techniques for high-resolution current recording from cells and cell-free membrane patches. *Pflugers Arch*, **391,** 85-100.

HAN, J., TRUELL, J., GNATENCO, C. & KIM, D. (2002). Characterization of four types of background potassium channels in rat cerebellar granule neurons. *J Physiol*, **542,** 431-44.

HARA, Y., KITAMURA, K. & KURIYAMA, H. (1980). Actions of 4-aminopyridine on vascular smooth muscle tissues of the guinea-pig. *Br J Pharmacol*, **68,** 99-106.

HARDIN, C.D. & VALLEJO, J. (2006). Caveolins in vascular smooth muscle: form organizing function. *Cardiovasc Res*, **69,** 808-15.

HASUNUMA, K., RODMAN, D.M. & MCMURTRY, I.F. (1991). Effects of K^+ channel blockers on vascular tone in the perfused rat lung. *Am Rev Respir Dis*, **144,** 884-7.

HILLE, B. (1986). Ionic channels: molecular pores of excitable membranes. *Harvey Lect*, **82,** 47-69.

HIRATA, Y., TAKAGI, Y., FUKUDA, Y. & MARUMO, F. (1989). Endothelin is a potent mitogen for rat vascular smooth muscle cells. *Atherosclerosis*, **78,** 225-8.

HOHENEGGER, M., SUKO, J., GSCHEIDLINGER, R., DROBNY, H. & ZIDAR, A. (2002). Nicotinic acid-adenine dinucleotide phosphate activates the skeletal muscle ryanodine receptor. *Biochem J*, **367,** 423-31.

HONG, Z., WEIR, E.K., NELSON, D.P. & OLSCHEWSKI, A. (2004). Subacute hypoxia decreases voltage-activated potassium channel expression and function in pulmonary artery myocytes. *Am J Respir Cell Mol Biol*, **31,** 337-43.

HSU, K., SEHARASEYON, J., DONG, P., BOUR, S. & MARBAN, E. (2004). Mutual functional destruction of HIV-1 Vpu and host TASK-1 channel. *Mol Cell*, **14,** 259-67.

HULME, J.T., COPPOCK, E.A., FELIPE, A., MARTENS, J.R. & TAMKUN, M.M. (1999). Oxygen sensitivity of cloned voltage-gated K^+ channels expressed in the pulmonary vasculature. *Circ Res*, **85,** 489-97.

HYNYNEN, M.M. & KHALIL, R.A. (2006). The vascular endothelin system in hypertension--recent patents and discoveries. *Recent Pat Cardiovasc Drug Discov*, **1,**

95-108.

INOUE, Y., OIKE, M., NAKAO, K., KITAMURA, K. & KURIYAMA, H. (1990). Endothelin augments unitary calcium channel currents on the smooth muscle cell membrane of guinea-pig portal vein. *J Physiol*, **423,** 171-91.

IVY, D.D., LE CRAS, T.D., HORAN, M.P. & ABMAN, S.H. (1998). Increased lung preproET-1 and decreased ET_B-receptor gene expression in fetal pulmonary hypertension. *Am J Physiol*, **274,** L535-41.

KANG, D., HAN, J. & KIM, D. (2006). Mechanism of inhibition of TREK-2 (K_{2P}10.1) by the Gq-coupled M_3 muscarinic receptor. *Am J Physiol Cell Physiol*, **291,** C649-56.

KANG, D., HAN, J., TALLEY, E.M., BAYLISS, D.A. & KIM, D. (2004). Functional expression of TASK-1/TASK-3 heteromers in cerebellar granule cells. *J Physiol*, **554,** 64-77.

KIM, D. (2003). Fatty acid-sensitive two-pore domain K^+ channels. *Trends Pharmacol Sci*, **24,** 648-54.

KIM, D., FUJITA, A., HORIO, Y. & KURACHI, Y. (1998). Cloning and functional expression of a novel cardiac two-pore background K^+ channel (cTBAK-1). *Circ Res*, **82,** 513-8.

KIM, Y., BANG, H. & KIM, D. (2000). TASK-3, a new member of the tandem pore K^+ channel family. *J Biol Chem*, **275,** 9340-7.

KUMAR, P., KAZZI, N.J. & SHANKARAN, S. (1996). Plasma immunoreactive endothelin-1 concentrations in infants with persistent pulmonary hypertension of the newborn. *Am J Perinatol*, **13,** 335-41.

LEI, Q., JONES, M.B., TALLEY, E.M., GARRISON, J.C. & BAYLISS, D.A. (2003). Molecular

mechanisms mediating inhibition of G protein-coupled inwardly-rectifying K^+ channels. *Mol Cells*, **15,** 1-9.

LEONOUDAKIS, D., GRAY, A.T., WINEGAR, B.D., KINDLER, C.H., HARADA, M., TAYLOR, D.M., CHAVEZ, R.A., FORSAYETH, J.R. & YOST, C.S. (1998). An open rectifier potassium channel with two pore domains in tandem cloned from rat cerebellum. *J Neurosci*, **18,** 868-77.

LESAGE, F. & LAZDUNSKI, M. (2000). Molecular and functional properties of two-pore-domain potassium channels. *Am J Physiol Renal Physiol*, **279,** F793-801.

LOPES, C.M., GALLAGHER, P.G., BUCK, M.E., BUTLER, M.H. & GOLDSTEIN, S.A. (2000). Proton block and voltage gating are potassium-dependent in the cardiac leak channel KCNK3. *J Biol Chem*, **275,** 16969-78.

LOPES, C.M., ROHACS, T., CZIRJAK, G., BALLA, T., ENYEDI, P. & LOGOTHETIS, D.E. (2005). PIP_2 hydrolysis underlies agonist-induced inhibition and regulates voltage gating of two-pore domain K^+ channels. *J Physiol*, **564,** 117-29.

MAINGRET, F., PATEL, A.J., LAZDUNSKI, M. & HONORE, E. (2001). The endocannabinoid anandamide is a direct and selective blocker of the background K^+ channel TASK-1. *Embo J*, **20,** 47-54.

MATHIE, A. (2007). Neuronal two-pore-domain potassium channels and their regulation by G protein-coupled receptors. *J Physiol*, **578,** 377-85.

MEDHURST, A.D., RENNIE, G., CHAPMAN, C.G., MEADOWS, H., DUCKWORTH, M.D., KELSELL, R.E., GLOGER, II & PANGALOS, M.N. (2001). Distribution analysis of human two pore domain potassium channels in tissues of the central nervous system and periphery. *Brain Res Mol Brain Res*, **86,** 101-14.

MEUTH, S.G., BUDDE, T., KANYSHKOVA, T., BROICHER, T., MUNSCH, T. & PAPE, H.C. (2003). Contribution of TWIK-related acid-sensitive K^+ channel 1 (TASK1) and TASK3 channels to the control of activity modes in thalamocortical neurons. *J Neurosci*, **23,** 6460-9.

MILLAR, J.A., BARRATT, L., SOUTHAN, A.P., PAGE, K.M., FYFFE, R.E., ROBERTSON, B. & MATHIE, A. (2000). A functional role for the two-pore domain potassium channel TASK-1 in cerebellar granule neurons. *Proc Natl Acad Sci U S A*, **97,** 3614-8.

MIYAUCHI, T., YORIKANE, R., SAKAI, S., SAKURAI, T., OKADA, M., NISHIKIBE, M., YANO, M., YAMAGUCHI, I., SUGISHITA, Y. & GOTO, K. (1993). Contribution of endogenous endothelin-1 to the progression of cardiopulmonary alterations in rats with monocrotaline-induced pulmonary hypertension. *Circ Res*, **73,** 887-97.

MIYOSHI, Y., NAKAYA, Y., WAKATSUKI, T., NAKAYA, S., FUJINO, K., SAITO, K. & INOUE, I. (1992). Endothelin blocks ATP-sensitive K^+ channels and depolarizes smooth muscle cells of porcine coronary artery. *Circ Res*, **70,** 612-6.

NAKAJIMA, T., HAZAMA, H., HAMADA, E., WU, S.N., IGARASHI, K., YAMASHITA, T., SEYAMA, Y., OMATA, M. & KURACHI, Y. (1996). Endothelin-1 and vasopressin activate Ca^{2+}-permeable non-selective cation channels in aortic smooth muscle cells: mechanism of receptor-mediated Ca^{2+} influx. *J Mol Cell Cardiol*, **28,** 707-22.

NAKANISHI, K., TAJIMA, F., NAKATA, Y., OSADA, H., TACHIBANA, S., KAWAI, T., TORIKATA, C., SUGA, T., TAKISHIMA, K., AURUES, T. & IKEDA, T. (1999). Expression of endothelin-1 in rats developing hypobaric hypoxia-induced pulmonary hypertension. *Lab Invest*, **79,** 1347-57.

NEHER, E. (1992). Nobel lecture. Ion channels for communication between and within cells. *Neuron*, **8,** 605-12.

NEHER, E. & SAKMANN, B. (1976). Single-channel currents recorded from membrane of denervated frog muscle fibres. *Nature*, **260,** 799-802.

NELSON, M.T. & QUAYLE, J.M. (1995). Physiological roles and properties of potassium channels in arterial smooth muscle. *Am J Physiol*, **268,** C799-822.

O'CONNELL, A.D., MORTON, M.J. & HUNTER, M. (2002). Two-pore domain K^+ channels-molecular sensors. *Biochim Biophys Acta*, **1566,** 152-61.

O'KELLY, I., BUTLER, M.H., ZILBERBERG, N. & GOLDSTEIN, S.A. (2002). Forward transport. 14-3-3 binding overcomes retention in endoplasmic reticulum by dibasic signals. *Cell*, **111,** 577-88.

OLSCHEWSKI, A., HONG, Z., NELSON, D.P. & WEIR, E.K. (2002). Graded response of K^+ current, membrane potential, and $[Ca^{2+}]_i$ to hypoxia in pulmonary arterial smooth muscle. *Am J Physiol Lung Cell Mol Physiol*, **283,** L1143-50.

OLSCHEWSKI, A., LI, Y., TANG, B., HANZE, J., EUL, B., BOHLE, R.M., WILHELM, J., MORTY, R.E., BRAU, M.E., WEIR, E.K., KWAPISZEWSKA, G., KLEPETKO, W., SEEGER, W. & OLSCHEWSKI, H. (2006). Impact of TASK-1 in human pulmonary artery smooth muscle cells. *Circ Res*, **98,** 1072-80.

OONUMA, H., NAKAJIMA, T., NAGATA, T., IWASAWA, K., WANG, Y., HAZAMA, H., MORITA, Y., YAMAMOTO, K., NAGAI, R. & OMATA, M. (2000). Endothelin-1 is a potent activator of nonselective cation currents in human bronchial smooth muscle cells. *Am J Respir Cell Mol Biol*, **23,** 213-21.

OSIPENKO, O.N., EVANS, A.M. & GURNEY, A.M. (1997). Regulation of the resting potential of rabbit pulmonary artery myocytes by a low threshold, O_2-sensing potassium current.

Br J Pharmacol, **120,** 1461-70.

PARK, W.S., KO, E.A., HAN, J., KIM, N. & EARM, Y.E. (2005). Endothelin-1 acts via protein kinase C to block K_{ATP} channels in rabbit coronary and pulmonary arterial smooth muscle cells. *J Cardiovasc Pharmacol*, **45,** 99-108.

PATEL, A.J. & HONORE, E. (2001). Molecular physiology of oxygen-sensitive potassium channels. *Eur Respir J*, **18,** 221-7.

PATEL, A.J., HONORE, E., LESAGE, F., FINK, M., ROMEY, G. & LAZDUNSKI, M. (1999). Inhalational anesthetics activate two-pore domain background K^+ channels. *Nat Neurosci*, **2,** 422-6.

PATEL, A.J. & LAZDUNSKI, M. (2004). The 2P-domain K^+ channels: role in apoptosis and tumorigenesis. *Pflugers Arch*, **448,** 261-73.

PATEL, A.J., LAZDUNSKI, M. & HONORE, E. (1997). Kv2.1/Kv9.3, a novel ATP-dependent delayed-rectifier K^+ channel in oxygen-sensitive pulmonary artery myocytes. *Embo J*, **16,** 6615-25.

PENG, W., HOIDAL, J.R. & FARRUKH, I.S. (1999). Role of a novel KCa opener in regulating K^+ channels of hypoxic human pulmonary vascular cells. *Am J Respir Cell Mol Biol*, **20,** 737-45.

PENG, W., MICHAEL, J.R., HOIDAL, J.R., KARWANDE, S.V. & FARRUKH, I.S. (1998). ET-1 modulates KCa-channel activity and arterial tension in normoxic and hypoxic human pulmonary vasculature. *Am J Physiol*, **275,** L729-39.

PLATOSHYN, O., REMILLARD, C.V., FANTOZZI, I., MANDEGAR, M., SISON, T.T., ZHANG, S., BURG, E. & YUAN, J.X. (2004). Diversity of voltage-dependent K^+ channels in human

pulmonary artery smooth muscle cells. *Am J Physiol Lung Cell Mol Physiol*, **287,** L226-38.

PONGS, O. (1992). Molecular biology of voltage-dependent potassium channels. *Physiol Rev*, **72,** S69-88.

POST, J.M., GELBAND, C.H. & HUME, J.R. (1995). $[Ca^{2+}]_i$ inhibition of K^+ channels in canine pulmonary artery. Novel mechanism for hypoxia-induced membrane depolarization. *Circ Res*, **77,** 131-9.

POST, J.M., HUME, J.R., ARCHER, S.L. & WEIR, E.K. (1992). Direct role for potassium channel inhibition in hypoxic pulmonary vasoconstriction. *Am J Physiol*, **262,** C882-90.

RAJAN, S., WISCHMEYER, E., XIN LIU, G., PREISIG-MULLER, R., DAUT, J., KARSCHIN, A. & DERST, C. (2000). TASK-3, a novel tandem pore domain acid-sensitive K^+ channel. An extracellular histiding as pH sensor. *J Biol Chem*, **275,** 16650-7.

REYES, R., DUPRAT, F., LESAGE, F., FINK, M., SALINAS, M., FARMAN, N. & LAZDUNSKI, M. (1998). Cloning and expression of a novel pH-sensitive two pore domain K^+ channel from human kidney. *J Biol Chem*, **273,** 30863-9.

RUBIN, L.J., BADESCH, D.B., BARST, R.J., GALIE, N., BLACK, C.M., KEOGH, A., PULIDO, T., FROST, A., ROUX, S., LECONTE, I., LANDZBERG, M. & SIMONNEAU, G. (2002). Bosentan therapy for pulmonary arterial hypertension. *N Engl J Med*, **346,** 896-903.

SANDERS, K.M. & KOH, S.D. (2006). Two-pore-domain potassium channels in smooth muscles: new components of myogenic regulation. *J Physiol*, **570,** 37-43.

SHIMODA, L.A., SYLVESTER, J.T., BOOTH, G.M., SHIMODA, T.H., MEEKER, S., UNDEM, B.J. & SHAM, J.S. (2001). Inhibition of voltage-gated K^+ currents by endothelin-1 in human

pulmonary arterial myocytes. *Am J Physiol Lung Cell Mol Physiol*, **281,** L1115-22.

SHIMODA, L.A., SYLVESTER, J.T. & SHAM, J.S. (1998). Inhibition of voltage-gated K^+ current in rat intrapulmonary arterial myocytes by endothelin-1. *Am J Physiol*, **274,** L842-53.

SIROIS, J.E., LEI, Q., TALLEY, E.M., LYNCH, C., 3RD & BAYLISS, D.A. (2000). The TASK-1 two-pore domain K^+ channel is a molecular substrate for neuronal effects of inhalation anesthetics. *J Neurosci*, **20,** 6347-54.

STEWART, D.J., LEVY, R.D., CERNACEK, P. & LANGLEBEN, D. (1991). Increased plasma endothelin-1 in pulmonary hypertension: marker or mediator of disease? *Ann Intern Med*, **114,** 464-9.

SUH, B.C., HOROWITZ, L.F., HIRDES, W., MACKIE, K. & HILLE, B. (2004). Regulation of KCNQ2/KCNQ3 current by G protein cycling: the kinetics of receptor-mediated signaling by Gq. *J Gen Physiol*, **123,** 663-83.

TALLEY, E.M. & BAYLISS, D.A. (2002). Modulation of TASK-1 (KCNK3) and TASK-3 (KCNK9) potassium channels: volatile anesthetics and neurotransmitters share a molecular site of action. *J Biol Chem*, **277,** 17733-42.

TALLEY, E.M., SIROIS, J.E., LEI, Q. & BAYLISS, D.A. (2003). Two-pore-Domain (KCNK) potassium channels: dynamic roles in neuronal function. *Neuroscientist*, **9,** 46-56.

VADASZ, I., MORTY, R.E., KOHSTALL, M.G., OLSCHEWSKI, A., GRIMMINGER, F., SEEGER, W. & GHOFRANI, H.A. (2005). Oleic acid inhibits alveolar fluid reabsorption: a role in acute respiratory distress syndrome? *Am J Respir Crit Care Med*, **171,** 469-79.

VAN RENTERGHEM, C. & LAZDUNSKI, M. (1993). Endothelin and vasopressin activate low

conductance chloride channels in aortic smooth muscle cells. *Pflugers Arch*, **425,** 156-63.

VON BETHMANN, A.N., BRASCH, F., NUSING, R., VOGT, K., VOLK, H.D., MULLER, K.M., WENDEL, A. & UHLIG, S. (1998). Hyperventilation induces release of cytokines from perfused mouse lung. *Am J Respir Crit Care Med*, **157,** 263-72.

WANG, J., JUHASZOVA, M., RUBIN, L.J. & YUAN, X.J. (1997). Hypoxia inhibits gene expression of voltage-gated K^+ channel alpha subunits in pulmonary artery smooth muscle cells. *J Clin Invest*, **100,** 2347-53.

WANSTALL, J.C. (1996). The pulmonary vasodilator properties of potassium channel opening drugs. *Gen Pharmacol*, **27,** 599-605.

WEIR, E.K. & ARCHER, S.L. (1995). The mechanism of acute hypoxic pulmonary vasoconstriction: the tale of two channels. *Faseb J*, **9,** 183-9.

WEIR, E.K. & OLSCHEWSKI, A. (2006). Role of ion channels in acute and chronic responses of the pulmonary vasculature to hypoxia. *Cardiovasc Res*, **71,** 630-41.

WEISSMANN, N., DIETRICH, A., FUCHS, B., KALWA, H., AY, M., DUMITRASCU, R., OLSCHEWSKI, A., STORCH, U., MEDEROS Y SCHNITZLER, M., GHOFRANI, H.A., SCHERMULY, R.T., PINKENBURG, O., SEEGER, W., GRIMMINGER, F. & GUDERMANN, T. (2006). Classical transient receptor potential channel 6 (TRPC6) is essential for hypoxic pulmonary vasoconstriction and alveolar gas exchange. *Proc Natl Acad Sci U S A*, **103,** 19093-8.

WILLIAMS, T.M. & LISANTI, M.P. (2004). The caveolin proteins. *Genome Biol*, **5,** 214.

WORT, S.J., WOODS, M., WARNER, T.D., EVANS, T.W. & MITCHELL, J.A. (2001). Endogenously released endothelin-1 from human pulmonary artery smooth muscle

promotes cellular proliferation: relevance to pathogenesis of pulmonary hypertension and vascular remodeling. *Am J Respir Cell Mol Biol*, **25,** 104-10.

YANAGISAWA, M., KURIHARA, H., KIMURA, S., TOMOBE, Y., KOBAYASHI, M., MITSUI, Y., YAZAKI, Y., GOTO, K. & MASAKI, T. (1988). A novel potent vasoconstrictor peptide produced by vascular endothelial cells. *Nature*, **332,** 411-5.

YOSHIBAYASHI, M., NISHIOKA, K., NAKAO, K., SAITO, Y., MATSUMURA, M., UEDA, T., TEMMA, S., SHIRAKAMI, G., IMURA, H. & MIKAWA, H. (1991). Plasma endothelin concentrations in patients with pulmonary hypertension associated with congenital heart defects. Evidence for increased production of endothelin in pulmonary circulation. *Circulation*, **84,** 2280-5.

YU, Y., PLATOSHYN, O., ZHANG, J., KRICK, S., ZHAO, Y., RUBIN, L.J., ROTHMAN, A. & YUAN, J.X. (2001). c-Jun decreases voltage-gated K^+ channel activity in pulmonary artery smooth muscle cells. *Circulation*, **104,** 1557-63.

YUAN, X.J. (1995). Voltage-gated K^+ currents regulate resting membrane potential and $[Ca^{2+}]_i$ in pulmonary arterial myocytes. *Circ Res*, **77,** 370-8.

ZAMORA, M.A., DEMPSEY, E.C., WALCHAK, S.J. & STELZNER, T.J. (1993). BQ123, an ET_A receptor antagonist, inhibits endothelin-1-mediated proliferation of human pulmonary artery smooth muscle cells. *Am J Respir Cell Mol Biol*, **9,** 429-33.

10.2. Figure Index

10.3. Table Index

Summary

The characteristics of the two pore-domain potassium channel and its modulation by endothelin-1 (ET-1) were tested by means of the whole-cell patch-clamp technique combined with TASK-1 small interfering RNA (siRNA) in primary human pulmonary arterial smooth muscle cells. We have found that the TASK-1 protein is present in primary hPASMC via immunofluorescence and immunoprecipitation methods. PCR studies detect only TASK-1 mRNA in primary and cultured hPASMC.

Under whole cell voltage-clamp conditions, noninactivating K^+ current is clearly but reversibly inhibited by anandamide, which is a direct and selective TASK-1 channel blocker. Its inhibition induces a significant membrane depolarization. As a consequence of the inhibition of the outward current, anandamide also influences the reversal potential of the current. The anandamide sensitive current is reversed close to -84 mV, the calculated Nernst equilibrium potential for K^+ under these conditions. Moreover, under symmetrical K^+ conditions in the same cell, anandamide causes a clear inhibition of the K^+ current. The anandamide sensitive current is linear and reversed at or near 0 mV, the calculated Nernst equilibrium potential for K^+ under these conditions. We have found that the TASK-1 channels are their extreme sensitive to variations in the extracellular pH. It behaves in a pH dependent manner in primary hPASMC across the full voltage range. A pH of 8.3 significantly hyperpolarizes the cells, whereas acidification causes a membrane depolarization in primary hPASMC (-10±1 mV versus 13±2 mV; n=5).

By assessing the O_2 sensitivity of this channel in primary hPASMC, under current-clamp conditions, we have found that hypoxia causes a marked cell depolarization (by 10±1 mV; n=9) and that the hypoxia-sensitive current reverses close to -84 mV.

Further investigations, using the TASK-1 small interfering RNA (siRNA) technique show that TASK-1 knockdown causes a depolarization of the resting membrane potential compared to control cells (-26±1 mV versus -40±2 mV; $P<0.05$). Pretreatment of hPASMC with TASK-1 siRNA results in a lack of significant further suppression of the

I_{KN} by anandamide, acidosis, hypoxia, or ET-1.

In order to detect the modulation by ET-1, we have found that ET-1 markedly reduces the TASK-1 current in primary hPASMCs and significantly and dose-dependently depolarizes hPASMCs. The concentration-response curve calculation shows that IC_{50} is 1.6 ± 0.3 nM (n = 5). The effect of ET-1 on the TASK-1 current is completely abolished by a pre-application of 10 µM anandamide or a pH of 6.3. The ET-1-sensitive current is reversed close to -84 mV, the calculated Nernst equilibrium potential for K^+ under these conditions. Application of isoflurane (1mM) enhances the TASK-1 current, and this facilitation is blocked by ET-1.

In order to investigate the possible physiological relevance of TASK-1 for the ET-1 induced pulmonary vasoconstriction, the ET-1-induced pressor response in the isolated perfused mouse lungs was carried out. ET-1 induces a dose-dependent increase in the PA pressure. The PA vasoconstriction is more pronounced when anandamide is given prior to ET-1. The application of 8 nM ET-1 increases PAP with 15.6 ± 2.3 mmHg. When anandamide is given prior to ET-1, the increase is 23.8 ± 1.0 mmHg (n =5).

To investigate the possible involvement of the ET-1-mediated signal transduction in human PASMCs, we have employed different signaling molecular blockers and demonstrated that the endothelin-sensitivity of TASK-1 requires ET_A receptors, phospholipase C (PLC), phosphatidylinositol 4,5-biphosphate (PIP_2), diacylglycerol (DAG) and protein kinase C (PKC) in hPASMCs. However, caveolins are not involved in this process. Additionally, ET-1 stimulates the threonine phosphorylation of TASK-1, but not its tyrosine phosphorylation.

Our results suggest that TASK-1 is expressed in human PASMC and is hypoxia-sensitive. Furthermore, TASK-1 is regulated by ET-1 involved in ET_A-PLC-PIP_2-DAG-PKC pathway at clinically relevant concentrations, which might represent a novel pathological mechanism related to pulmonary arterial hypertension.

Zusammenfassung

In dieser Arbeit wurden die Effekte von Endothelin-1 (ET-1) am two-pore domain Kaliumkanal TASK-1 von humanen primären pulmonalarteriellen glatten Muskelzellen (PASMCs) geprüft. Für die Untersuchungen wurde die Patch-Clamp Methode mit der small interfering RNA Methode kombiniert.

Mittels pharmakologischen Tools wurde der TASK-1 Kaliumkanal, der auch als Hintergrundkaliumkanal bezeichnet wird, in der Ganzzell-Konfiguration der Patch-Clamp Methode untersucht. Der nicht-inaktivierende Kaliumstrom des TASK-1 Kanals wurde durch Anandamide (spezifischer Blocker von TASK-1), durch extrazelluläre Azidose und durch Hypoxie inhibiert. Die Anwendung der small interfering RNA gegen TASK-1 führte zu einer Inhibierung des TASK-1 Stromes und zu einem Verlust der Effekte von Anandamide, Azidose und Hypoxie sowie zu einer signifikanten Depolarisation des Membranpotentials der humanen PASMCs (-26±1 mV vs. -40±2 mV; $P<0.05$). Die Existenz von TASK-1 wurde auch mittels PCR und Immunhistochemie bestätigt.

Der sehr effektive Vasokonstriktor Endothelin-1 blockierte den TASK-1 Kanal in klinisch relevanten Konzentrationen signifikant. Der Effekt war dosisabhängig mit einer halb-maximalen Konzentration (IC_{50}) von 1.6 ± 0.3 nM. Die Effekte von ET-1 am TASK-1 Kanal wurden durch Vorapplikation von Anadamide oder Azidose aufgehoben. Die Anwendung von ET-1 führte zu einer signifikanten Vasokonstriktion in den Pulmonalarterien in der isoliert-perfundierten Mauslunge.

Weitere Untersuchungen zeigten, dass für die Effekte von ET-1 der Endothelinrezeptor A, die Aktivierung von Phospholipase C (PLC), Phosphatidylinositol 4,5-biphosphate (PIP_2), Diacylglycerol (DAG) und Proteinkinase C (PKC) in humanen PASMCs essentiell sind.

Diese Ergebnisse zeigen, dass TASK-1 für die Effekte von ET-1 eine zentrale Bedeutung hat und daher einen neuen Signalweg repräsentiert, der für die Entstehung der pulmonalen Hypertonie, aber auch für mögliche therapeutische Ansätze eine wichtige Rolle spielen könnte.

Acknowledgments

I would like to extend my sincere gratitude to
my supervisor, Prof. Andrea Olschewski,
for her instructive advice and useful suggestions about my thesis,
and her help in the completion of this thesis;

to Prof. Dr. Horst Olschewski
for his professional consultation, support and
indefatigable care for my experimental work;

Prof. Dr. Norbert Weissmann and Dr. Rory E. Morty
for their help and support;

Colleagues from the team: Yingji Li, Chandran Nagaraj and Zoltán Bálint
for their consultations and support;

Brigitte Agari, Sabine Gräf-Höchst,
Christiane Hild, Maria M. Stein,
Alexandra Hof, Maria Schloffer,
Karin Quanz and Elisabeth Wirnsperger
for their excellent technical assistance;

All the other tutors and teachers
for their direct and indirect help.

Der Lebenslauf wurde aus der elektronischen Version der Arbeit entfernt.

The curriculum vitae was removed from the electronic version of the paper.